

Award Number:

W81XWH-07-1-0448

TITLE:

Structural and Mechanistic Analyses of TSC1/2 and Rheb 1/2-Mediated Regulation of the mTORC Pathway

PRINCIPAL INVESTIGATOR:

PI: David M. Sabatini, M.D./Ph.D.

CONTRACTING ORGANIZATION:

Whitehead Institute for Biomedical Research

Cambridge, MA 02142-1493

REPORT DATE:

July 2009

TYPE OF REPORT:

Annual Report

PREPARED FOR: U.S. Army Medical Research and Materiel Command
Fort Detrick, Maryland 21702-5012

DISTRIBUTION STATEMENT:

X Approved for public release; distribution unlimited

The views, opinions and/or findings contained in this report are those of the author(s) and should not be construed as an official Department of the Army position, policy or decision unless so designated by other documentation.

REPORT DOCUMENTATION PAGE			<i>Form Approved</i> <i>OMB No. 0704-0188</i>		
Public reporting burden for this collection of information is estimated to average 1 hour per response, including the time for reviewing instructions, searching existing data sources, gathering and maintaining the data needed, and completing and reviewing this collection of information. Send comments regarding this burden estimate or any other aspect of this collection of information, including suggestions for reducing this burden to Department of Defense, Washington Headquarters Services, Directorate for Information Operations and Reports (0704-0188), 1215 Jefferson Davis Highway, Suite 1204, Arlington, VA 22202-4302. Respondents should be aware that notwithstanding any other provision of law, no person shall be subject to any penalty for failing to comply with a collection of information if it does not display a currently valid OMB control number. PLEASE DO NOT RETURN YOUR FORM TO THE ABOVE ADDRESS.					
1. REPORT DATE (DD-MM-YYYY) 01-07-2009		2. REPORT TYPE Annual Report		3. DATES COVERED (From - To) 07/01/2008 - 06/30/2009	
4. TITLE AND SUBTITLE Structural and Mechanistic Analyses of TSC1/2 and Rheb 1/2-Mediated Regulation of the mTORC Pathway.			5a. CONTRACT NUMBER		
			5b. GRANT NUMBER W81XW-07-1-0448		
			5c. PROGRAM ELEMENT NUMBER		
6. AUTHOR(S) David M. Sabatini, M.D., Ph.D. Seong Woo A. Kang, Ph.D. Yasemin Sancak			5d. PROJECT NUMBER		
			5e. TASK NUMBER		
			5f. WORK UNIT NUMBER		
7. PERFORMING ORGANIZATION NAME(S) AND ADDRESS(ES) Whitehead Institute for Biomedical Research Cambridge, MA 02142-1493			8. PERFORMING ORGANIZATION REPORT NUMBER		
9. SPONSORING / MONITORING AGENCY NAME(S) AND ADDRESS(ES) US Army Medical Research and Material Command Fort Detrick, MD 21702-5013			10. SPONSOR/MONITOR'S ACRONYM(S)		
			11. SPONSOR/MONITOR'S REPORT NUMBER(S)		
12. DISTRIBUTION / AVAILABILITY STATEMENT Approved for public release; distribution unlimited					
13. SUPPLEMENTARY NOTES					
14. ABSTRACT The mammalian target of rapamycin complex 1 (mTORC1) formed by mTOR, Raptor, mLST8 and PRAS40 is a principal regulator of cell growth in response to the nutrient and energy status of the cell, and its deregulation has recently emerged as a key driver in human cancers. Here, we present three-dimensional structures of the intact complex, as well as free Raptor, at nominal resolutions of 26Å and 30Å, as determined by cryo-electron microscopy (cryo-EM). The molecular architecture of the holoenzyme contains a two-fold symmetry, suggesting mTORC1 as an obligate dimeric complex. It is characterized by a flat and rhomboid shape that features a central cavity and peripheral protrusions. Antibody labeling and molecular docking revealed that the smaller subunits mLST8 and PRAS40 localize to the periphery and constitute the distal "feet-like" structures and the central "tips," respectively. In addition, in the intact complex, mTOR and Raptor form a dimeric interface that is disrupted acutely by rapamycin treatment. Dimeric particles accommodate rapamycin at a distal site that is independent of the Raptor-binding region. While binding of a single FKBP12-rapamycin complex has no observable effects on the structural integrity of mTORC1, extended incubation <i>in vitro</i> results in fast and complete disintegration of the complex. Consistent with this observation, loss of the structural integrity of mTORC1 manifests a differential regulation of 4E-BP1 and S6K1 phosphorylation by rapamycin both <i>in vivo</i> and <i>in vitro</i> .					
15. SUBJECT TERMS mTOR, mTORC1, raptor, TSC, Rheb, Rag, rapamycin, cryo-EM					
16. SECURITY CLASSIFICATION OF:			17. LIMITATION OF ABSTRACT UU	18. NUMBER OF PAGES 21	19a. NAME OF RESPONSIBLE PERSON USAMRMC
a. REPORT U	b. Abstract U	c. THIS PAGE U			19b. TELEPHONE NUMBER (include area code)

Table of Contents

	<u>Page</u>
Introduction.....	4
Body.....	4
Key Research Accomplishments.....	9
Reportable Outcomes.....	9
Conclusion.....	9
References.....	9
Appendices.....	11

INTRODUCTION

The multi-protein kinase mTORC1 (mammalian target of rapamycin complex 1) regulates cell growth by coordinating upstream signals from growth factors, intracellular energy levels, and amino acid availability and is deregulated in diseases such as cancer and diabetes. The TSC1/2 complex is the main convergence point of many upstream regulatory signals in the mTORC1 signaling network, with the notable exception of amino acid availability. TSC1/2 is a GTPase activating protein (GAP) for the small GTPase Rheb, which binds directly to mTORC1 and stimulates its activity when GTP-bound. In response to growth factor withdrawal or energy stress, activation of TSC1/2 leads to mTORC1 inhibition by decreasing Rheb-GTP levels. In contrast to growth factor signaling, the mechanism of regulation of mTORC1 activity in response to amino acids is poorly understood and puzzling. Although Rheb is necessary for mTORC1 activation, high Rheb-GTP levels achieved by TSC2 loss or Rheb over-expression have different effects on amino acid signaling to mTORC1. While in TSC2 null state cells still respond to amino acid stimulation, Rheb over-expression makes the pathway insensitive to amino acid starvation. Although the mechanism of this difference is not known, it points to the presence of other players in amino acid signaling. Given that the mTOR pathway is an important target in TSC treatment, understanding how impairment of TSC1/2 function results in the activation of mTORC1 is critical. In particular, there is a lack of information about the nutrient and growth factor input to the mTORC1 complex and the inhibitory mechanism of rapamycin. With the long-term goal of developing anti-cancer therapeutics based on mTORC1 regulatory mechanisms, our structural and biochemical studies aim to find efficient means of regulating the mTOR signaling network. Therefore, we propose structural analysis of mTORC1 as well as mechanistic analysis of mTORC1 activation via Rheb.

BODY

Aim 1: Understand the role of Rheb-mediated phosphorylation of Raptor in the regulation of mTORC1

Recently, the identification of Rag GTPases as components of in amino acid signaling to mTORC1 provided new insight. Mammals have four Rag GTPases (RagA-D) that form two different functional classes in terms of mTORC1 signaling. RagA and RagB activate mTORC1 when GTP-bound as opposed to RagC and RagD, which have an inhibitory effect on mTORC1 when GTP-bound (1). Amino acid stimulation induces GTP loading of RagB, which enables a direct interaction between Raptor component of mTORC1 and Rag GTPases. As a result of amino acid stimulation, mTORC1 localizes to Rab7 positive membranes, and this translocation is dependent on the presence of Rag GTPases as well as Raptor. When either is knocked down by RNAi, mTOR localization change and activation by amino acid stimulation are prevented.

Intracellular localization of mTORC1 is now accepted to be a major determinant of its activity, however, the identity of the membranes that mTORC1 associates with is still poorly defined. Previously we showed that mTOR changes its cellular localization from cytoplasm to Rab7 positive membranes in response to amino acid stimulation. Because Rab7 marks both late endosomes and lysosomes, we used lysosome associated membrane protein (LAMP), a lysosome specific protein, to unambiguously identify these membranes. Surprisingly, we found that mTORC1 associates with lysosomes in response to amino acids, and Rag GTPases are also lysosome-associated proteins, but unlike mTORC1, their intracellular localization is not affected by amino acid availability (Figure 1).

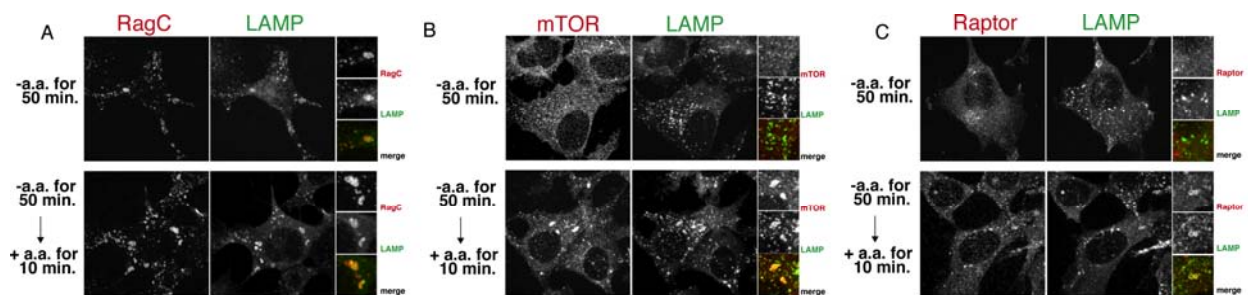


Figure 1. mTORC1 pathway proteins associate with lysosomes. (a) RagC localizes to lysosomes independent of amino acid availability (b) mTOR and (c) Raptor associate with lysosomes in the presence of amino acids only.

Given the importance of TSC1/2 complex and Rheb in activation of mTORC1, we investigated whether TSC2 or Rheb loss affect mTORC1 localization in response to amino acids. Neither TSC2 loss nor Rheb knock-down by RNAi altered mTORC1 localization, although activation of mTORC1 was blunted when Rheb was knocked-down (Figures 2).

Our results clearly showed that Rheb does not regulate mTORC1 localization, however, it is required for amino acid-induced mTORC1 activation. We proposed that these observations could be explained by a model where Rag GTPases localize mTORC1 to lysosomal membranes in the presence of amino acids, enabling mTORC1-Rheb contact and mTORC1 activation. One major prediction of this model would be that if mTORC1 can be constitutively localized to lysosomes, its activity should be independent of amino acid availability.

In order to test this model, we targeted mTORC1 to lysosomes by adding Rheb localization sequence (the last 15 amino acids of Rheb) to the carboxyl terminus of Raptor. This small modification in Raptor was sufficient to localize mTORC1 to lysosomes independent of amino acid availability (Figure 3A). Most importantly, as predicted by our model, expression of lysosome-targeted Raptor made the mTORC1 pathway insensitive to amino acid starvation (Figure 3B).

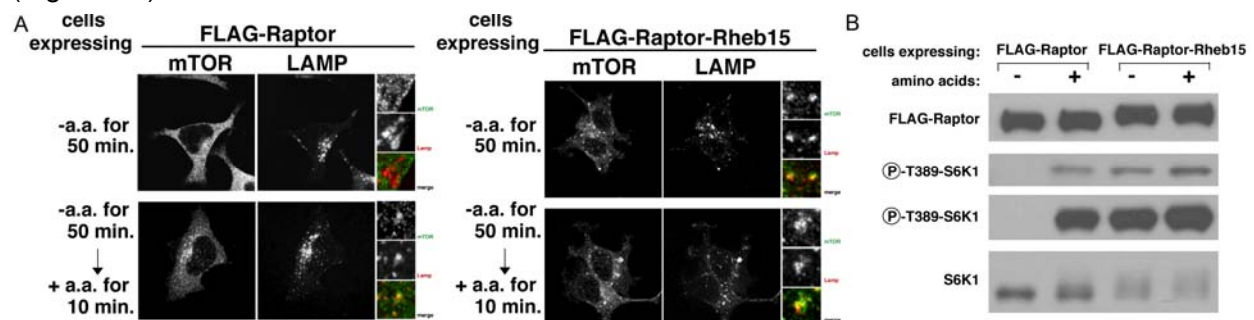


Figure 3. Addition of Rheb localization sequence to Raptor is sufficient to mediate mTORC1 signaling independent of amino acid availability. (a) Lysosomal mTOR localization in response to Rheb15 sequence. (b) Constitutive lysosomal localization of Raptor makes the mTORC1 pathway insensitive to amino acid starvation

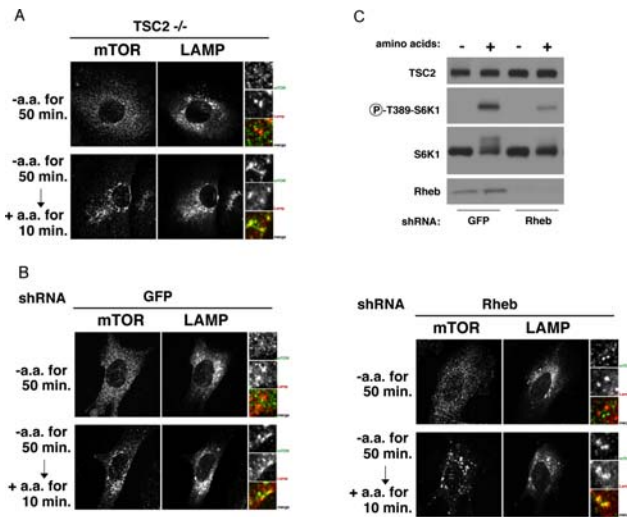


Figure 2. TSC1/2 and Rheb do not regulate mTORC1 localization in response to amino acids. (a) Lysosomal mTOR localization in response to amino acid stimulation is independent of TSC2. (b) Lysosomal mTOR localization in response to amino acid stimulation is independent of Rheb.

Aim 2: Elucidate the structural features of mTORC1 and its interacting proteins via X-ray crystallography, cryo-EM and SAXS

mTOR is an evolutionarily conserved serine/threonine kinase that integrates environmental cues and regulates cellular processes pertaining to cell growth, including mRNA translation, ribosome biogenesis, autophagy, and metabolism. In recent years, mTOR has emerged as a critical component of the oncogenic phosphoinositide 3-kinase (PI3K) signaling pathway (2), and due to its prominent role in tumor growth, understanding the structural features of mTOR is crucial for the rational development of mTOR inhibitors (3). mTOR participates in two structurally and functionally distinct signaling complexes, mTOR complex 1 (mTORC1) and mTOR complex 2 (mTORC2). mTORC1, which consists of mTOR, Raptor, mLST8, and PRAS40, is acutely sensitive to inhibition by the small molecule rapamycin, and promotes cell autonomous growth in part through two downstream substrates, S6 kinase 1 (S6K1) and the translational inhibitor eIF-4E-binding protein 1 (4E-BP1). Phosphorylation of both proteins promotes the upregulation of cell growth machinery through their influence on cap-dependent translation (4-7).

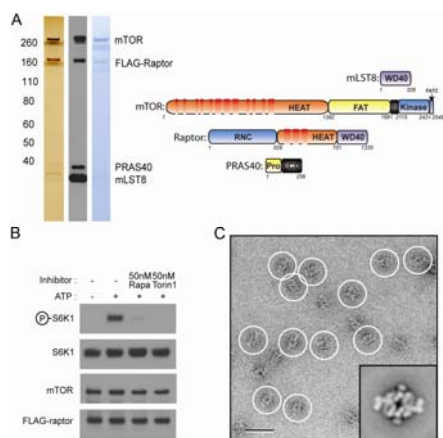


Figure 4. mTORC1 purification. (a) SDS-PAGE and western blot analyses of mTORC1 components and their predicted domain structures. (b) *In vitro* kinase assay. (c) EM of negatively stained mTORC1 (scale bar = 50 nm).

cell line stably expressing N-terminal FLAG-tagged Raptor, we purified mTORC1 by anti-FLAG agarose and gel filtration chromatography (Figure 1A). In addition to SDS-PAGE analysis, purified fractions were analyzed by mass spectrometry to confirm the presence of the known mTORC1 components, and the biochemical activity of the complex was assessed by *in vitro* kinase assays (Figure 1B). EM images of purified mTORC1 in negative stain revealed particles homogeneous in size and shape (Figure 1C). Projection averages calculated from a classification of 10,080 particle images illustrated that mTORC1 has an elongated, rhomboid shape with “feet-like” protrusions emanating from both ends of the molecule and features a central cavity (Figure 1C). The averages displayed a two-fold symmetry, providing evidence for the obligate dimeric organization of mTORC1 that had been previously proposed by genetic and co-immunoprecipitation studies (8-10).

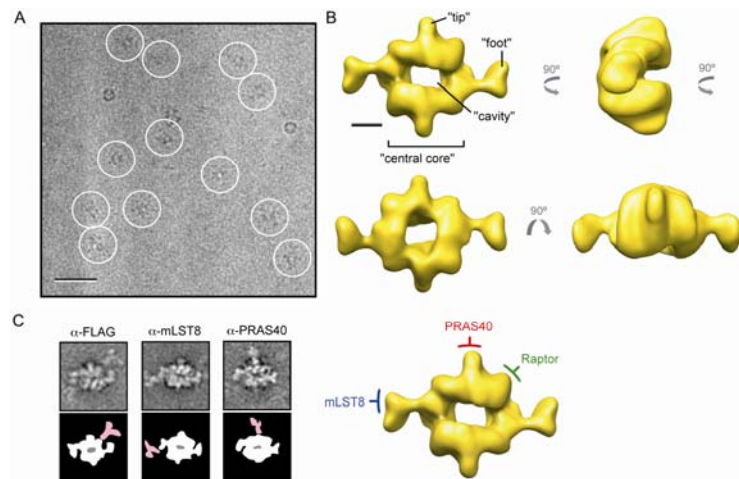


Figure 5. Cryo-EM reconstruction of mTORC1 and molecular organization. (a) Image of a vitrified specimen showing individual mTORC1 particles (scale bar = 50 nm). (b) Different views of the 3D reconstruction of mTORC1 low-pass filtered to 26 Å. (c) Molecular organization of mTORC1 predicted by antibody labeling.

sufficient number of particles for structure determination. The carbon film also induced mTORC1 to adsorb to the grid in a preferred orientation, making it necessary to collect images of tilted specimens to obtain the multiple views needed for a 3D reconstruction. The final data set

mTOR is a member of the family of phosphoinositide 3-kinase-related kinases (PIKK), and due to its large size and multiple interacting proteins, the overall architecture and subunit organization of mTORC1 are poorly understood (4). Furthermore, the specific roles of the various components of mTORC1 and how they collectively confer to the regulation of the intact complex remains unclear. To gain a better understanding of the structural features of mTORC1, we developed a method to purify human mTORC1, and applied EM approaches to assess its structure. Our purification method overcomes a number of key issues that complicate efforts to obtain homogeneous mTORC1, including: (1) mTORC1 is large and often does not survive isolation, preventing extensive biochemical analysis; (2) mTORC1 is defined by several conserved domains that nucleate multiple protein-protein interactions, hindering the homogeneity and proper folding of the purified protein; (3) mTORC1 requires an adequate expression system that can accommodate the expression of endogenous mTOR interacting proteins and their post-translational modifications. Utilizing a HEK293T

To determine the three-dimensional (3D) structure of mTORC1, we produced a reliable initial model by calculating a random conical tilt (RCT) reconstruction with 50°/0° tilt pair images of cryo-negatively stained specimens. Collecting images of vitrified mTORC1 specimens initially proved difficult due to low protein concentration (attempts to concentrate mTORC1 samples were unsuccessful) and strong tendency of mTORC1 to dissociate upon contact with the air-water interface. We overcame these difficulties by adsorbing mTORC1 to a thin carbon film prior to vitrification. Even so only a few particles were present (Figure 2A), requiring us to collect a large number of images to obtain a

contained 28,325 particle images, including 3,905 from 45° tilted specimens. A 3D reconstruction was calculated by aligning these individual images to the initial model produced with the cryo-negatively stained sample, followed by iterative refinement of their orientation parameters. An estimated resolution of the final reconstruction is 26 Å according to the Fourier shell correlation = 0.5 criterion. However, the resolution is clearly anisotropic, with lower resolution in the direction perpendicular to the carbon film, a result of the limited number of views other than the face-on view. mTORC1 has overall dimensions of approximately 290Å x 210Å x 135Å (Figure 2B). Assuming that there are two subunits of each of the four components, a fully assembled mTORC1 has a calculated molecular mass of 1MDa, which is consistent with the estimated volume of the reconstruction (approximately $1.4 \times 10^6 \text{ \AA}^3$ at the contour level of the displayed map).

The cryo-EM structure of the central cavity reveals an oval shape when viewed from one face, but a rectangular shape from the opposite face, with two troughs located at the extensions linking the central core to the “feet-like” structures. While the biological relevance of this cavity remains elusive, this finding is significant considering how structurally dynamic mTORC1 appears to be. Hence, its location between the two monomeric complexes may enable substrates such as 4E-BP1 to shuttle between the two mTOR active sites within mTORC1. Consistent with this idea, 4E-BP1 has multiple mTORC1 phosphorylation sites (11). Alternatively, the central cavity may support a structural flexibility of the complex to facilitate mTOR autophosphorylation (12). Because its size (~40 Å x 28 Å) is large enough to accommodate double-stranded DNA (dsDNA), another, albeit less likely, possibility is that the cavity may serve as a docking platform for nucleic acids. While mTORC1 has not yet been shown to interact with dsDNA, several members of the PIKK family, most notably DNA-PK, are known to mediate DNA repair by directly binding to dsDNA (13).

While the cryo-EM structure revealed the overall shape of mTORC1, at the current resolution it was impossible to define intermolecular and intersubunit boundaries. Therefore, we performed antibody labeling experiments to localize individual subunits within mTORC1, including Raptor (FLAG), mLST8, and PRAS40. The particles were imaged by negative stain EM and analyzed by classification and image averaging. We discovered that mLST8 localizes to the distal “foot-like” structures, PRAS40 to the small tips in the mid-section of the central core, and Raptor to the corner of the core (Figure 2C). The occasional observation of double-labeled particles provided further assurance for the dimeric organization of mTORC1.

Interestingly, the FLAG-tagged Raptor that did not incorporate into mTORC1 eluted as a separate peak from gel filtration (Figure 3A). Negative stain EM showed that purified Raptor is homogeneous in size and shape (Figure 3B). The 3D reconstruction of Raptor, determined by the RCT approach using 60°/0° image pairs of negatively stained specimens revealed that its overall shape resembles a “comma” with the circular lobe likely representing the predicted C-terminal WD40 domain (Figure 3C). Utilizing the antibody labeling data as a guide, the structure of mTORC1 provides an adequate framework in which the EM-reconstruction of Raptor can be meaningfully fitted (gold surface in Figure 3D). By subtracting two copies of Raptor, the densities

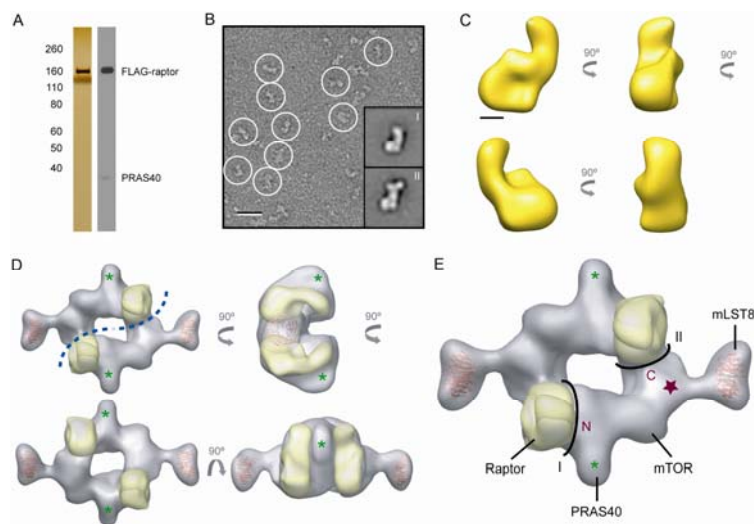


Figure 6. 3D reconstruction of Raptor and molecular docking. (a) Purification of Raptor. (b) EM image of negatively stained Raptor (scale bar = 25 nm). (c) Different views of the Raptor 3D reconstruction (scale bar = 2.5 nm). (d) Molecular docking. Two copies of the Raptor 3D reconstruction (gold) and two models of a representative WD40 domain (PDB code 3EMH, red) were placed into the cryo-EM density map (gray). The green asterisk depicts the location of PRAS40 as determined by antibody labeling. The blue dotted line represents the dimer interface. (e) The proposed locations of the N- and C-terminal domains (marked “N” and “C”) and the kinase domain of mTOR (purple star).

occupied by two mTOR subunits can be predicted, while accounting for a minor contribution by mLST8. mLST8, an obligate binding partner of mTOR, is solely composed of a single WD40 motif, and according to our antibody labeling experiment, we docked two WD40 models (PDB code 3EMH) into our cryo-EM map (red ribbon diagram in Figure 3D). Lastly, PRAS40 is located at the central tips in mTORC1 (indicated by green asterisk in Figure 3D). After detecting these three subunits, we reasoned that the remaining unassigned density must represent mTOR, which would occupy the space between the two Raptor molecules, forming two distinct interfaces (labeled I and II in Figure 3E). Because mLST8 is known to interact near the C-terminal kinase domain of mTOR, we suspect that the kinase domain is adjacent to the “foot” (indicated by the purple star in Figure 3E). From the position of the kinase domain, we deduce that the N-terminus of mTOR interacts with the flat face of one Raptor molecule, forming interface I, whereas the C-terminus interacts with the side of the second Raptor molecule (Figure 3E), forming interface II. This arrangement agrees with previous domain mapping studies, which show that Raptor associates with the N-terminal HEAT repeats and the C-terminal FAT domain of mTOR. These interlocking Raptor-mTOR interactions within the central core provide an understanding of the basis of dimerization and illustrate the crucial function of Raptor in mediating and maintaining the higher-order organization of mTORC1. The peripheral location of mLST8, which only contacts one mTOR molecule, may help mediate substrate entry into the catalytic site and/or “lock” the mTOR kinase domain into a specific conformation required for activity. However, mLST8 may not be crucial in preserving the kinase function of mTORC1, as evidenced by mLST8 deficient mice, since it is not required to maintain the integrity of the mTOR-Raptor interaction. Finally, our model suggests that PRAS40 localizes in close proximity to Raptor (asterisk in Figure 3D), which is in agreement with the known binding of PRAS40 to Raptor. Interestingly, some class averages of purified Raptor showed an additional, small density, which may represent bound PRAS40. This interpretation is supported by Western blots, showing PRAS40 to be present in the analyzed Raptor fraction (Figure 3A).

With a more detailed understanding of the molecular architecture and subunit organization of mTORC1, we next investigated how rapamycin inhibits mTOR kinase activity. As an allosteric inhibitor of mTORC1, rapamycin requires the intracellular protein FKBP12 to form a gain-of-function complex, which directly interacts with the FKBP12-rapamycin-binding (FRB) domain of mTOR (14). A crystal structure of FKBP12-rapamycin in complex with the FRB domain of mTOR was previously reported (15). However, it remains unclear how this interaction prevents phosphorylation of direct mTOR substrates. Other biochemical studies indicate that the interaction between FKBP12-rapamycin and mTORC1 induces a conformational change that weakens the mTOR-Raptor interaction (5,6). To test this hypothesis, we incubated mTORC1 with N-terminal GST-tagged FKBP12 in the presence of 50nM rapamycin for 15 minutes, and then visualized the particles by negative stain EM. Although raw images did not reveal any obvious structural changes, image classification showed that about 10% of the particles had an additional density tethered to the region we assigned to mTOR and directly opposite of Raptor, likely constituting FKBP12-rapamycin (Figure 4A). Interestingly, we did not observe individual particles or averages of mTORC1 showing two extra densities, suggesting that either mTORC1 cannot accommodate two rapamycin complexes or this intermediate is short lived.

While acute exposure to FKBP12-rapamycin did not affect the structural integrity of mTORC1, extended incubations resulted in a drastic reduction in the total number of intact mTORC1 particles. Many smaller fragments appeared in the background, suggesting that FKBP12-rapamycin may cause a disassembly of mTORC1 (Figure 4B,C). Once initiated, this dissociation appeared to be swift, as we were unable to detect intermediates with defined structures during the course of the reaction. After one hour of incubation, no intact mTORC1 particles could be detected, and the sample contained only disordered fragments, likely representing free mTOR or its subcomplexes and undefined aggregates (Figure 4B,C).

The mechanism of rapamycin-mediated inhibition of mTORC1 is a highly dynamic process. Previous co-immunoprecipitation experiments suggests that transformation of the physical assembly of mTORC1 is likely responsible for rapamycin’s effect on S6K1 and 4E-BP1 (16). Although structural perturbation of mTORC1 may be the primary cause of reduced

activation of S6K1 and 4E-BP1, at least *in vitro*, our observation that mTORC1 undergoes time-dependent disassembly upon rapamycin treatment indicates that the inhibitory mechanism is, perhaps, more complicated. Because mTORC1's substrates appear to exhibit different binding affinities for Raptor, effects of rapamycin on 4E-BP1 and S6K1 may also reflect a difference in time-dependence *in vivo* (16). To test this hypothesis, we treated HEK-293T cells with either rapamycin or Torin1, an ATP-competitive inhibitor of mTOR recently identified (17), and assessed the inhibition of S6K1 and 4E-BP1 phosphorylation over a period of two hours by immunoblotting (Figure 4D). As expected, both inhibitors led to very rapid loss of S6K1 phosphorylation within 5 minutes. However, rapamycin-induced inhibition of 4E-BP1 phosphorylation and concomitant association with eIF-4E occurred only after 30-60 minutes of rapamycin treatment in comparison to within minutes with Torin1 treatment.

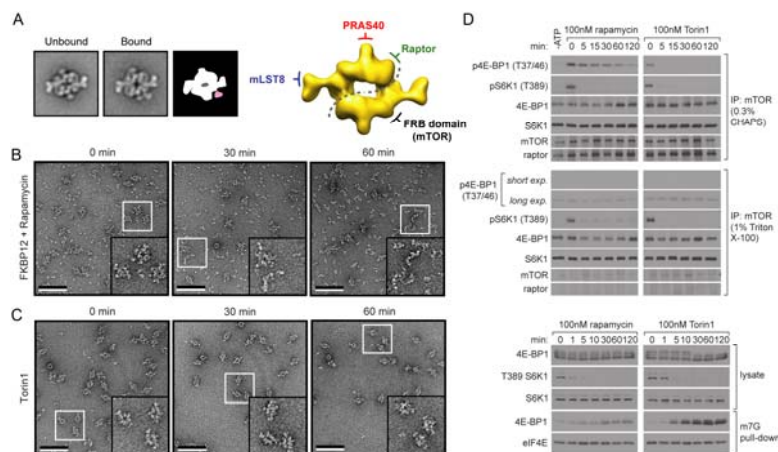


Figure 7. Effect of rapamycin-FKBP12 treatment. (a) Localization of the mTOR FKBP12-rapamycin binding (FRB) domain in mTORC1. (b) Time course study of rapamycin-FKBP12 treatment. The inset in each image shows an enlarged view of the area marked by the white square (scale bar = 100 nm). (c) Time course study of Torin1 treatment. (d) Inhibition of mTORC1 with rapamycin inhibits phosphorylation of 4E-BP1, not S6K1, in a time-dependent manner *in vivo* and *in vitro*.

affinities of two substrates for Raptor. It is known that S6K1 interacts more weakly with Raptor than 4E-BP1 does, suggesting that affinity may alter mTORC1's structure to allow the phosphorylation. To assess this latter assumption, we performed *in vitro* kinase assays using immuno-purified mTOR in the presence of Triton X-100, which completely disrupts Raptor-mTOR association (4,5). While mTORC1 with Raptor depleted can no longer facilitate the phosphorylation of 4E-BP1, S6K1 phosphorylation was not largely affected, suggesting that the mTOR kinase can catalyze phosphorylation of S6K1 with or without Raptor.

Based on these observations and our knowledge of the molecular organization of mTORC1, we propose the following model for FKBP12-rapamycin mediated inhibition of mTORC1. Initial binding of one FKBP12-rapamycin may cause a subtle conformational change in mTOR that weakens the essential mTOR-Raptor interactions, but does not suffice to disrupt the dimeric architecture. Moreover, the bound FKBP12-rapamycin may occlude substrate binding and/or block substrate access to the active site, resulting in short-term inhibition observed for the substrate S6K1. Over time, either amplified structural strain caused by first FKBP12-rapamycin or, perhaps, binding of the second rapamycin complex would lead to an instantaneous and complete disintegration of the already "weakened" mTORC1. Consequently, 4E-BP1, capable of withstanding minor structural alterations due to its relatively strong affinity for Raptor, may not present itself to mTORC1, and thus, 4E-BP1 phosphorylation is affected by rapamycin only when the complex is fully disassembled.

KEY RESEARCH ACCOMPLISHMENTS

- Characterized intracellular localization of mTORC1 pathway components
- Localized mTORC1 to different cellular membranes

Because the effect of rapamycin on 4E-BP1 was detected on a similar time-scale as mTORC1 dissociation observed upon FKBP12-rapamycin treatment in our EM analysis, we next measured the kinetics of rapamycin-induced 4E-BP1 dephosphorylation by *in vitro* kinase assays. Despite an obvious attenuation of S6K1 phosphorylation by rapamycin and Torin1 within 5 minutes of treatment, we determined the inhibition of recombinant 4E-BP1 by rapamycin to be highly time-dependent, requiring up to 60 minutes of incubation time (Figure 4D). We reason that this discrepancy could be a consequence of different binding

- Identified of a lysosome based signaling system that is important for amino acid signaling
- Developed purification methods for human mTORC1 and free Raptor
- Deciphered the structures of mTORC1 and free Raptor by cryo-EM
- Labeled mTORC1 with antibodies targeting Raptor, mLST8 and PRAS40
- Characterized the mechanism of mTORC1 inhibition by FKBP12-rapamycin
- Developed Torin1 as a highly potent and specific mTOR inhibitor

REPORTABLE OUTCOMES

- Thoreen, C.C., Kang, S.A., Chang, J.W., Liu, Q, Zhang, J., Gao, Y., Reichling, L.J., Sim, T. Sabatini, D.M., and Gray, N.S. An ATP-competitive mTOR inhibitor reveals rapamycin-insensitive functions of mTORC1. *J. Biol. Chem.* **2009**, 284 (12), 8023-8032.

CONCLUSION

Aim 1: Our results demonstrate conclusively for the first time that TSC1/2 and Rheb do not regulate mTORC1 localization, and that lysosomal localization of mTORC1 is necessary and sufficient for its activation by amino acids. Moreover, our results suggest the existence of a lysosome-based signaling system and implicate lysosomal membranes as the location of the amino acid sensor of the mTORC1 pathway.

Aim 2: For years, lack of meaningful structural information of the mTOR complexes has prevented us from answering a number of key questions concerning the mechanism of the action of the mTOR kinase, kinase-substrate interactions, and ultimately, its inhibition by FKBP12-rapamycin. Our cryo-EM structure of mTORC1 reveals that the holoenzyme exists as an obligate heterodimer, in which Raptor provides a basis for the complex assembly in part by scaffolding mTOR through its multiple protein-protein interfaces. Even though the exact structural dynamics of mTORC1 with regard to kinase activity remain elusive, the gross conformational changes associated with rapamycin binding are critical for the substrate-specific inhibition of mTORC1.

REFERENCES

1. Shaw, R.J., Cantley, L.C. Ras, PI(3)K and mTOR signaling controls tumour cell growth. *Nature* **2006**, 441, 424-30.
2. Guertin, D.A., Sabatini, D.M. Defining the role of mTOR in cancer. *Cancer Cell* **2007**, 12, 9-22.
3. Sarbassov, D.D., Ali, S.M., Sabatini, D.M. Growing roles for the mTOR pathway. *Curr Opin Cell Biol* **2005**, 17, 596-603.
4. Kim, D.-H., Sarbassov, D., Ali, S.M., King, J.E., Latek, R.R., Erdjument-Bromage, H., Tempst, P., Sabatini, D.M. mTOR interacts with raptor to form a nutrient-sensitive complex that signals to the growth machinery. *Cell* **2002**, 110 163-175.
5. Kim, D.-H., Sarbassov, D., Ali, S.M., Latek, R.R., Erdjument-Bromage, H., Tempst, P., Sabatini, D.M. GbL: a positive regulator of the rapamycin-sensitive pathway required for the nutrient-sensitive interaction between mTOR and raptor. *Mol Cell* **2003**, 11, 895-904.
6. Sancak, Y., Thoreen, C.C., Peterson, T.R., Lindquist, R.A., Kang, S.A., Spooner, E., Carr, S.A., Sabatini, D.M. PRAS40 Is an Insulin-Regulated Inhibitor of the mTORC1 Protein Kinase. *Mol Cell* **2007**, 25, 903-915.
7. Wang, L, Rhodes, C.J., Lawrence, J.C. Jr. Activation of mammalian target of rapamycin (mTOR) by insulin is associated with stimulation of 4EBP1 binding to dimeric mTOR complex 1. *J Biol Chem* **2006**, 281, 24293-303.
8. Takahara, T., Hara, K., Yonezawa, K., Sorimachi, H., Maeda, T. Nutrient-dependent multimerization of the mammalian target of rapamycin through the N-terminal HEAT repeat region. *J Biol Chem.* **2006**, 281, 28605-14.
9. Zhang, Y., Billington, C.J. Jr., Pan, D., Neufeld, T.P. Drosophila Target of Rapamycin Kinase Functions as a Multimer. *Genetics*, **2006**; 172, 355-362.

11. Fingar, D.C., Salama, S., Tsou, C., Harlow, E., Blenis, J. Mammalian cell size is controlled by mTOR and its downstream targets S6K1 and 4E-BP1/eIF4E. *Genes Dev* **2002**, 16,1472-87.
12. Acosta-Jaquez, H.A., Keller, J.A., Foster, K.G., Ekim, B., Soliman, G.A., Ballif, B.A., Fingar, D.C. Site-specific mTOR phosphorylation promotes mTORC1-mediated signaling and cell growth. *Mol Cell Biol.* **2009**, 29, 4308-4324.
13. Adami, A., Garcia-Alvarez, B., Arias-Palomo, E., Barford, D., Llorca, O. Structure of TOR and its complex with KOG1. *Mol Cell* **2007**, 27, 509-16.
14. Burnett, P.E., Barrow, R.K., Cohen, N.A., Snyder, S.H., Sabatini, D.M. RAFT1 phosphorylation of the translational regulators p70 S6 kinase and 4E-BP1. *Proc Natl Acad Sci USA* **1998**, 95,1432-7.
15. Choi, J., Chen, J., Schreiber, S.L., Clardy, J. Structure of the FKBP12-rapamycin complex interacting with the binding domain of human FRAP. *Science* **1996**, 273, 239-42.
16. Choo, A.Y., Blenis, J. Not all substrates are treated equally: implications for mTOR, rapamycin-resistance and cancer therapy. *Cell Cycle* **2009**, 8, 567-72.
17. Thoreen, C.C., Kang, S.A., Chang, J.W., Liu, Q, Zhang, J., Gao, Y., Reichling, L.J., Sim, T. Sabatini, D.M., Gray, N.S. An ATP-competitive mTOR inhibitor reveals rapamycin-insensitive functions of mTORC1. *J. Biol. Chem.* **2009**, 284 (12), 8023-8032.

An ATP-competitive Mammalian Target of Rapamycin Inhibitor Reveals Rapamycin-resistant Functions of mTORC1^{*[5]}

Received for publication, January 15, 2009 Published, JBC Papers in Press, January 15, 2009, DOI 10.1074/jbc.M900301200

Carson C. Thoreen^{‡§}, Seong A. Kang^{‡§}, Jae Won Chang[¶], Qingsong Liu[¶], Jianming Zhang[¶], Yi Gao[¶], Laurie J. Reichling[¶], Taebo Sim[¶], David M. Sabatini^{‡§**1}, and Nathanael S. Gray^{¶1,2}

From the [‡]Whitehead Institute for Biomedical Research, Cambridge, Massachusetts 02142, [§]Howard Hughes Medical Institute, Department of Biology and ^{**}Koch Center for Integrative Cancer Research, Massachusetts Institute of Technology, Cambridge, Massachusetts 02139, [¶]Department of Cancer Biology, Dana Farber Cancer Institute, Department of Biological Chemistry and Molecular Pharmacology, Harvard Medical School, Boston, Massachusetts 02115, and ^{||}Invitrogen Corporation, Madison, Wisconsin 53719

The mammalian target of rapamycin (mTOR) kinase is the catalytic subunit of two functionally distinct complexes, mTORC1 and mTORC2, that coordinately promote cell growth, proliferation, and survival. Rapamycin is a potent allosteric mTORC1 inhibitor with clinical applications as an immunosuppressant and anti-cancer agent. Here we find that Torin1, a highly potent and selective ATP-competitive mTOR inhibitor that directly inhibits both complexes, impairs cell growth and proliferation to a far greater degree than rapamycin. Surprisingly, these effects are independent of mTORC2 inhibition and are instead because of suppression of rapamycin-resistant functions of mTORC1 that are necessary for cap-dependent translation and suppression of autophagy. These effects are at least partly mediated by mTORC1-dependent and rapamycin-resistant phosphorylation of 4E-BP1. Our findings challenge the assumption that rapamycin completely inhibits mTORC1 and indicate that direct inhibitors of mTORC1 kinase activity may be more successful than rapamycin at inhibiting tumors that depend on mTORC1.

The mammalian target of rapamycin (mTOR)³ pathway is considered a major regulator of cell growth. The mTOR serine/

threonine kinase is the founding component of the pathway and the catalytic subunit of two functionally distinct protein complexes, mTORC1 and mTORC2. mTORC1 contains the large protein Raptor, as well as mLST8/GβL and PRAS40, whereas mTORC2 is defined by the protein Rictor and also includes Sin1, Protor, and mLST8/GβL (1). Growth factors, such as insulin and IGF, activate both complexes, and they are important downstream effectors of the PI3K/PTEN signaling network (2). Additionally, the availability of nutrients, like amino acids and glucose, regulates mTORC1.

Many insights into mTOR signaling have come from investigations into the mechanism of action of rapamycin, a bacterially produced macrolide inhibitor of mTOR that has diverse clinical applications as an anti-fungal, immunosuppressant, and anti-cancer drug (3). Rapamycin acts through an unusual allosteric mechanism that requires binding to its intracellular receptor, FKBP12, for inhibition of its target. Under acute treatment, rapamycin is thought to selectively inhibit mTORC1, which is often referred to as the rapamycin-sensitive complex. Conversely, mTORC2 is considered rapamycin-insensitive, although its assembly can be inhibited by prolonged rapamycin treatment in some cell types (4). Because of its perceived potency and selectivity, rapamycin is commonly used in research experiments as a test of the involvement of mTORC1 in a particular process.

Two downstream mTORC1 substrates that were identified, in part, by their sensitivity to rapamycin are the S6 kinases (S6K1 and S6K2) and the translational inhibitor 4E-BP1. Both proteins mediate important links between mTORC1 and the cell growth machinery, largely through their influence on cap-dependent translation (reviewed in Ref. 5). All nuclear-encoded mRNAs possess a 5',7-methyl guanosine cap, which is recognized and bound by the small protein eIF-4E. Under growth-promoting conditions, eIF-4E also associates with the large

* This work was supported, in whole or in part, by National Institutes of Health Grants R01 AI47389 and R01 CA103866. This work was also supported by start-up funding from the Dana Farber Cancer Institute, the Barr Foundation, and the Damon Runyon Cancer Research Foundation (to N. S. G.), Keck Foundation, LAM Foundation, and Department of Defense Grant W81XWH-07-1-0448 (to D. M. S.), and a fellowship from the American Cancer Society (to S. A. K.). The costs of publication of this article were defrayed in part by the payment of page charges. This article must therefore be hereby marked "advertisement" in accordance with 18 U.S.C. Section 1734 solely to indicate this fact.

[5] The on-line version of this article (available at <http://www.jbc.org>) contains supplemental Experimental Procedures, Figs. S1–S5, and an additional reference.

¹ To whom correspondence may be addressed: Whitehead Institute, 9 Cambridge Center, Cambridge, MA 02142. Tel.: 617-258-6407; Fax: 617-258-5213; E-mail: sabatini@wi.mit.edu.

² To whom correspondence may be addressed: Dept. of Biological Chemistry and Molecular Pharmacology, Harvard Medical School, 250 Longwood Ave., Boston, MA 02115. Tel.: 617-582-8590; Fax: 617-582-8615; E-mail: Nathanael_Gray@dfci.harvard.edu.

³ The abbreviations used are: mTOR, mammalian target of rapamycin; Raptor, regulatory associated protein of mTOR; Rictor, rapamycin-insensitive com-

panion of mTOR; PI3K, phosphatidylinositol 3-kinase; LC3, light chain 3; 4E-BP1, eIF4E-binding protein 1; eIF4E, eukaryotic initiation factor 4E; GβL, G-β subunit-like; MEF, mouse embryonic fibroblast; mTORC1, mTOR complex 1; mTORC2, mTOR complex 2; HEK, human embryonic kidney; DMSO, dimethyl sulfoxide; CHAPS, 3-[(3-cholamidopropyl)dimethylammonio]-1-propanesulfonic acid; ATM, ataxia telangiectasia, mutated; PI, phosphatidylinositol; BSA, bovine serum albumin; PBS, phosphate-buffered saline; shRNA, short hairpin RNA.

Rapamycin-resistant Functions of mTORC1

scaffolding protein eIF-4G, the eIF-4A helicase, and the eIF-4B regulatory protein, together forming the eIF-4F complex. This complex, in conjunction with the eIF3 preinitiation complex, delivers the mRNA to the 40 S ribosomal subunit and primes the translational apparatus. 4E-BP1 interferes with this process by binding to eIF-4E and preventing the formation of a functional eIF-4F complex. However, its ability to do this is blocked by phosphorylation at four sites, two of which are considered rapamycin-sensitive. S6K1 also plays a role in regulating translational initiation by phosphorylating the S6 protein of the 40 S ribosomal subunit and by stimulating eIF-4A helicase activity (6–8).

Despite the connections of mTORC1 to the translational machinery, the effects of rapamycin on mammalian cell growth and proliferation are, oddly, less severe than its effects in yeast. In *Saccharomyces cerevisiae*, rapamycin treatment induces a starvation-like state that includes a severe G₁/S cell cycle arrest and suppression of translation initiation to levels below 20% of nontreated cells (9). Moreover, in yeast rapamycin strongly promotes induction of autophagy (self-eating), a process by which cells consume cytoplasmic proteins, ribosomes, and organelles, such as mitochondria, to maintain a sufficient supply of amino acids and other nutrients (10).

The effects of rapamycin in mammalian cells are similar to those in yeast, but typically much less dramatic and highly dependent on cell type. For instance, rapamycin only causes cell cycle arrest in a limited number of cell types and has modest effects on protein synthesis (11–13). Moreover, rapamycin is a relatively poor inducer of autophagy, and it is often used in combination with LY294002, an inhibitor of PI3K and mTOR (14). These inconsistent effects may explain why, despite high expectations, rapamycin has had only limited success as a clinical anti-cancer therapeutic. We have hypothesized that the effectiveness of rapamycin against a particular cancer might be determined by its ability to inhibit mTORC2 in addition to mTORC1 (15). To test this hypothesis, we developed the ATP-competitive inhibitor Torin1 that suppresses both complexes. In contrast to rapamycin, Torin1 treatment recapitulates in mammalian cells many of the phenotypes caused by TOR inhibition in yeast. Surprisingly, however, we find that these effects are independent of mTORC2 and are instead caused by inhibition of rapamycin-resistant functions of mTORC1.

EXPERIMENTAL PROCEDURES

Materials—Reagents were obtained from the following sources: antibodies to phospho-Thr-389 S6K, phospho-Ser-473 Akt, phospho-Thr-308 Akt, pan-Akt, phospho-Thr-36/47 4E-BP1, phospho-Ser-65 4E-BP1, phospho-Thr-70 4E-BP1, 4E-BP1, α -tubulin, Raptor, eIF-4E, phospho-S51 eIF2 α , cyclin D1, cyclin D3 and p27/Kip1 from Cell Signaling Technology (note: we have not confirmed that the phospho-Thr-70 4E-BP1 antibody does not detect unphosphorylated 4E-BP1); antibodies to mTOR, S6K, and horseradish peroxidase-labeled anti-mouse, anti-goat, and anti-rabbit secondary antibodies from Santa Cruz Biotechnology; anti-Rictor antibodies from Bethyl Laboratories; FuGENE 6 and Complete Protease Mixture from Roche Applied Science; FLAG M2 antibody, FLAG M2-agarose, and ATP from Sigma; 7-methyl-GTP-Sepharose from GE

Healthcare; PI-103 from Calbiochem; NVP-BEZ235 from Axon Medchem; rapamycin from LC Laboratories; PI3K- α from Millipore/Upstate; CellTiter-Glo, DNA-PK, and DNA-PK peptide substrate from Promega; phosphatidylinositol and phosphatidylserine from Avanti Polar Lipids; EasyTagTM EXPRESS ³⁵S protein labeling mix and ATP [γ -³²P] EasyTide from PerkinElmer Life Sciences; Dulbecco's modified Eagle's medium from SAFC Biosciences; inactivated fetal calf serum from Invitrogen. p53^{-/-}/TSC2^{-/-} MEFs as well as p53^{-/-}/TSC2^{+/+} MEFs were kindly provided by David Kwiatkowski (Harvard Medical School) and cultured in Dulbecco's modified Eagle's medium with 10% inactivated fetal calf serum. p53^{-/-}/mLST8^{-/-} and p53^{-/-}/Rictor^{-/-} MEFs have been described (16). Torin1 was synthesized and purified in the Gray Laboratory and is available upon request.

Cell Lysis—Cells rinsed once with ice-cold PBS were lysed in ice-cold lysis buffer (40 mM HEPES, pH 7.4, 2 mM EDTA, 10 mM pyrophosphate, 10 mM glycerophosphate, and 0.3% CHAPS or 1% Triton X-100, and 1 tablet of EDTA-free protease inhibitors per 25 ml). The soluble fractions of cell lysates were isolated by centrifugation at 13,000 rpm for 10 min in a microcentrifuge.

Mammalian Lentiviral shRNAs—All shRNA vectors were obtained from the collection of The RNAi Consortium at the Broad Institute (17). These shRNAs are named with the numbers found at the RNAi Consortium public website: mouse Raptor shRNA, TRCN0000077472, NM_028898.1-3729s1c1; and mouse Rictor shRNA, TRCT0000037708, NM_030168.2-867s1c1. shRNA-encoding plasmids were co-transfected with the Δ VPR envelope and vesicular stomatitis virus G packaging plasmids into actively growing HEK-293T using FuGENE 6 transfection reagent as described previously (18, 19). Virus-containing supernatants were collected at 48 h after transfection and filtered to eliminate cells, and target cells were infected in the presence of 8 μ g/ml Polybrene. 24 h later, cells were selected with puromycin and analyzed on the 4th day after infection.

Metabolic Labeling—Cells were seeded in 6-well plates and grown overnight. Cells were then treated with appropriate compounds for 2.5 h, washed one time with cysteine/methionine-free Dulbecco's modified Eagle's medium, and then incubated in 2 ml of cysteine/methionine-free Dulbecco's modified Eagle's medium, 10% dialyzed inactivated fetal calf serum, compound, and 165 μ Ci (15 μ l, 11 mCi/ μ l) of EasyTagTM EXPRESS ³⁵S protein labeling mix. After 30 min, cells were lysed, and soluble fractions were isolated by centrifugation at 13,000 rpm for 10 min. To precipitate protein, lysates were spotted on Whatman filter paper, precipitated with 5% trichloroacetic acid, washed two times for 5 min in cold 10% trichloroacetic acid, washed two times for 2 min in cold ethanol, washed one time for 2 min in acetone, and air-dried at room temperature. The amount of ³⁵S incorporated into protein was measured using a Beckman LS6500 Scintillation Counter.

mTORC1 and mTORC2 in Vitro Kinase Assays—To produce soluble mTORC1, we generated HEK-293T cell lines that stably express N-terminally FLAG-tagged Raptor using vesicular stomatitis virus G-pseudotyped MSCV retrovirus. For mTORC2, we similarly generated HeLa cells that stably express N-terminally FLAG-tagged Protor-1. Both complexes were purified by

lysing cells in 50 mM HEPES, pH 7.4, 10 mM sodium pyrophosphate, 10 mM sodium β -glycerophosphate, 100 mM NaCl, 2 mM EDTA, 0.3% CHAPS. Cells were lysed at 4 °C for 30 min, and the insoluble fraction was removed by microcentrifugation at 13,000 rpm for 10 min. Supernatants were incubated with FLAG-M2 monoclonal antibody-agarose for 1 h and then washed three times with lysis buffer and once with lysis buffer containing a final concentration of 0.5 M NaCl. Purified mTORC1 was eluted with 100 μ g/ml 3 \times FLAG peptide in 50 mM HEPES, pH 7.4, 100 mM NaCl. Eluate can be aliquoted and stored at -80 °C. Substrates S6K1 and Akt1 were purified as described previously (16, 20). Kinase assays were performed for 20 min at 30 °C in a final volume of 20 μ l consisting of the kinase buffer (25 mM HEPES, pH 7.4, 50 mM KCl, 10 mM MgCl₂, 500 μ M ATP) and 150 ng of inactive S6K1 or Akt1 as substrates. Reactions were stopped by the addition of 80 μ l of sample buffer and boiled for 5 min. Samples were subsequently analyzed by SDS-PAGE and immunoblotting.

PI3K and hVps34 Assays—Cellular IC₅₀ values for PI3K α were determined using p53^{-/-}/mLST8^{-/-} MEFs. Cells were treated with vehicle or increasing concentrations of compound for 1 h and then lysed. Phosphorylation of Akt Thr-308 was monitored by immunoblotting using a phospho-specific antibody. *In vitro* IC₅₀ values for PI3K α were determined as described previously (21). Briefly, chloroform stocks of phosphatidylinositol (PI) and phosphatidylserine were combined in equimolar ratios, dried under nitrogen gas, resuspended in 50 mM HEPES, pH 7.4, 100 mM KCl, sonicated to clarity using a bath sonicator, and aliquoted and stored at -80 °C. For kinase assays, purified PI3K α was combined with 100 μ M phosphatidylserine/phosphatidylinositol, compound, and 10 μ Ci of [γ -³²P]ATP (100 μ M final concentration) in kinase buffer and incubated at 37 °C for 20 min. Reactions were stopped with 1 N HCl. Lipid was extracted with a 1:1 mixture of chloroform:methanol and separated on silica TLC plates. ³²P-Labeled phosphatidylinositol 3-phosphate was quantitated by PhosphorImager. hVps34 was purified as a glutathione S-transferase fusion protein from HEK-293T cells (22) and assayed using the same procedure.

ATM and DNA-PK—For DNA-PK kinase assays, purified DNA-PK was combined with DNA-PK peptide substrate (derived from the N-terminal sequence of p53), compound, and 10 μ Ci/reaction [γ -³²P]ATP (100 μ M final concentration) in kinase buffer and incubated for 10 min at 37 °C. Reactions were stopped with 1 N HCl and spotted onto P81 phosphocellulose squares. P81 squares were washed three times for 5 min in 0.75% phosphoric acid, and one time for 5 min in acetone, dried, and measured by scintillation counter. ATM *in vitro* kinase assays were performed according to previously published protocols (21).

Cell Size Determinations—Cells were seeded in 10-cm culture dishes, grown overnight, and subjected to appropriate treatment. 24 h later, cells were harvested by trypsinization in a 5-ml volume, diluted 1:20 with counting solution (Isoton II Diluent, Beckman Coulter), and cell diameters determined using a particle size counter (Coulter Z2, Beckman Coulter) with Coulter Z2 AccuComp software.

Cell Proliferation/Viability Assay—Cell viability was assessed with the CellTiter-Glo Luminescent Cell Viability Assay. On Day 0, 96-well plates were seeded with 500 cells per well and grown overnight. On Day 1, cells were treated with the appropriate compounds and subsequently analyzed on Days 3–5. For analysis, plates were incubated for 60 min at room temperature; 50 μ l of CellTiter-Glo reagent was added to each well, and plates were mixed on an orbital shaker for 12 min. Luminescence was quantified on a standard plate luminometer.

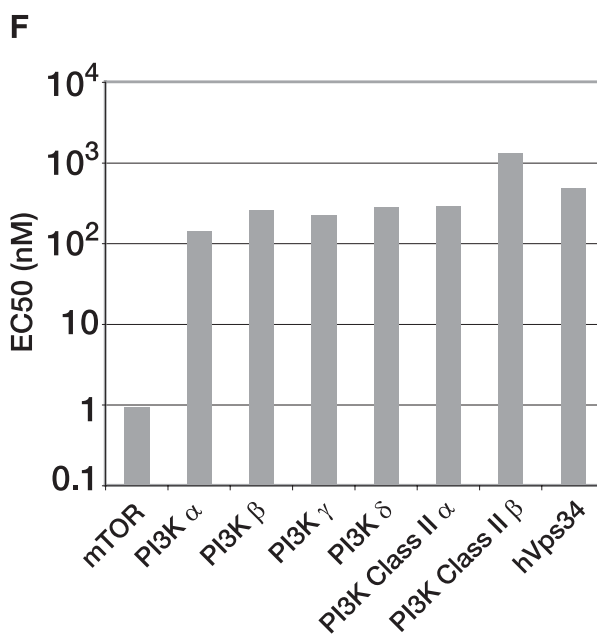
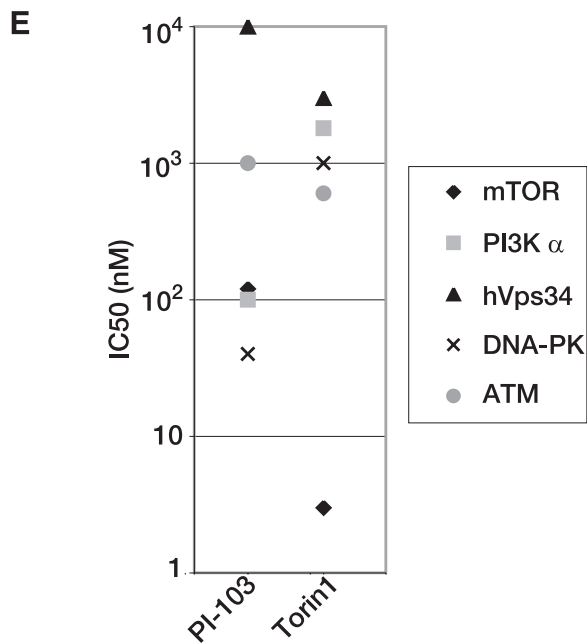
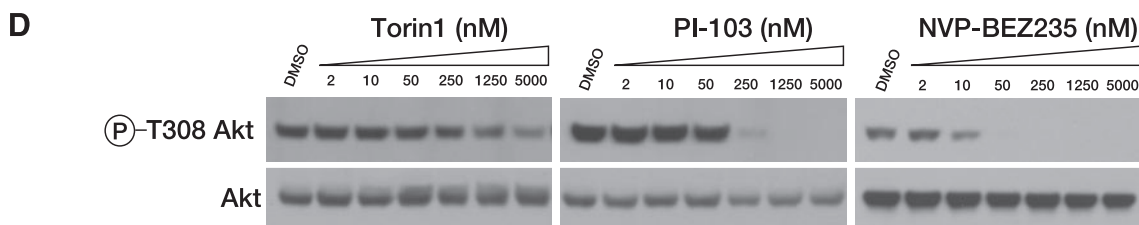
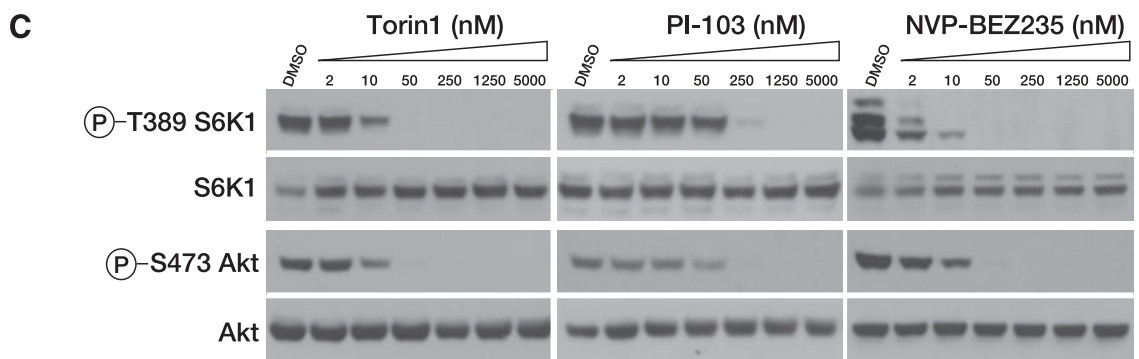
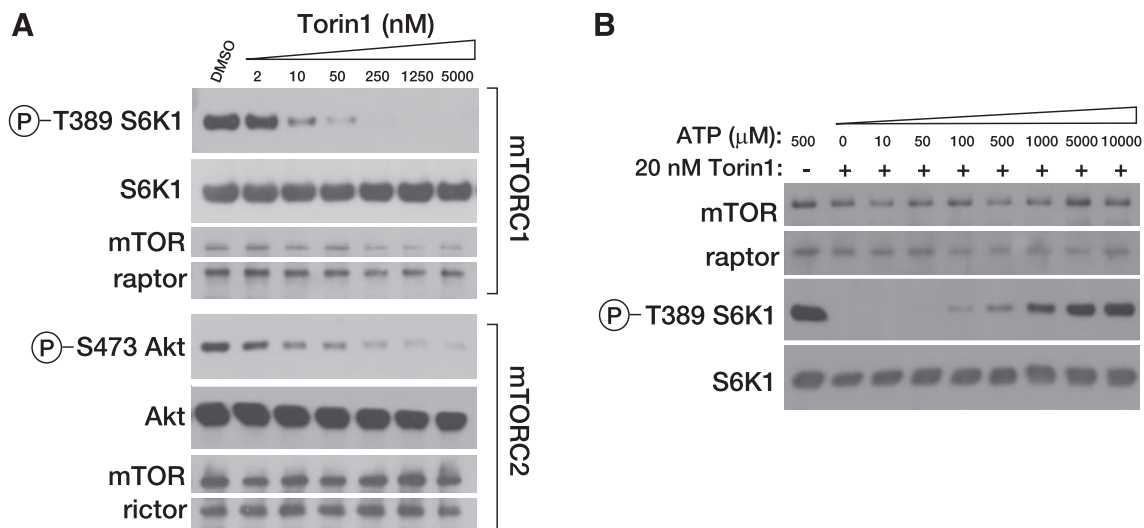
Cell Cycle Analysis—Cells were seeded in 15-cm plates and grown overnight. Cells were then subjected to the appropriate treatment for 48 h and then trypsinized, washed twice in PBS + 2% FBS, and then fixed overnight at 4 °C in ethanol. Cells were then washed three times in PBS + 1% BSA and incubated in PBS, 1% BSA, 50 μ g/ml propidium iodide, and 100 μ g/ml RNase at 37 °C for 30 min. Cells were then washed 1 \times in PBS + 1% BSA, resuspended in 1 ml PBS, and analyzed using a FACSCalibur flow cytometer (BD Biosciences). Cell cycle distribution was determined using the ModFit LT software package.

RESULTS

Torin1 Is a Potent and Selective mTOR Inhibitor—To identify small molecule ATP-competitive inhibitors of mTOR, we conducted a biochemical screen for inhibitors of mTOR kinase activity in a library of heterocyclic chemical compounds. From this screen, we identified a lead compound that was further elaborated through a medicinal chemistry effort to produce Torin1, a member of the pyridinonequinoline class of kinase inhibitors.⁴ In *in vitro* kinase assays using immuno-purified mTORC1 or mTORC2, Torin1 inhibits both mTOR-containing complexes with IC₅₀ values between 2 and 10 nM (Fig. 1A) and acts through an ATP-competitive mechanism (Fig. 1B). We also measured the potency of Torin1 in cells. MEFs were treated with increasing amounts of Torin1 or the dual mTOR/PI3K inhibitors PI-103 and NVP-BEZ235, and the activity of each complex was determined by monitoring the phosphorylation status of S6K at Thr-389 and Akt at Ser-473, mTORC1 and mTORC2 substrates, respectively (Fig. 1C). As *in vitro*, the IC₅₀ for Torin1 in cells is also between 2 and 10 nM. Unlike rapamycin, Torin1 had no effect on the stability of either mTORC1 or mTORC2.

We next determined the selectivity of Torin1 for mTOR over other kinases. Because mTOR belongs to the PI3K-like kinase family, a family of protein kinases that is defined by a high degree of homology to PI3K within the catalytic domain, many inhibitors of PI3K, such as wortmannin, LY294002, PI-103, and BEZ-235, are also reasonable mTOR inhibitors (21, 23, 24). To measure PI3K inhibition in cells, we made use of the observation that the phosphorylation of Akt at Thr-308 depends on two processes that directly reflect PI3K activity: phosphatidylinositol 3,4,5-triphosphate-dependent targeting of Akt to the plasma membrane and activation of PDK1, the kinase that directly phosphorylates this site. In wild-type cells, phosphorylation of Thr-308 is also influenced by phosphorylation at Ser-473 (19, 25, 26). To remove this latter variable, we tested compounds in MEFs where mLST8, an essential mTORC2

⁴ N. S. Gray, manuscript in preparation.



component, is deleted and Akt Ser-473 is constitutively dephosphorylated. Because Ser-473 is fixed in a single state in these cell lines, phosphorylation at Thr-308 only reflects PI3K activity. Using this system, we determined the cellular IC_{50} of Torin1 for PI3K to be $\sim 1.8 \mu M$ (Fig. 1D), nearly identical to our *in vitro* measurement of the IC_{50} for PI3K α (Fig. 1E). We also profiled our compound against other PI3K isoforms using the Adapta *in vitro* assay method, which confirmed a high degree of selectivity for mTOR (Fig. 1F).

Compounds that inhibit PI3K and mTOR also have the potential to inhibit other PI3K-like kinases, including the DNA-damage response kinases ATM and DNA-PK. For DNA-PK and ATM, we measured the IC_{50} of Torin1 using *in vitro* assays (Fig. 1E). We also measured inhibition of the Class III PI3K hVps34. Some reports have proposed that hVps34 acts upstream of mTORC1, and we wanted to be sure that cross-reactivity with this kinase was not indirectly influencing mTORC1 activity in cells (22). Torin1 was at least 200-fold selective for mTOR over each of these kinases. Finally, we screened Torin1 at a concentration of $10 \mu M$ against a panel of 353 diverse kinases using the Ambit Biosciences KinomeScan screening platform, which measures the relative binding of the target molecule to each kinase, and we found no indication of significant off-target effects (data shown in supplemental material). These results suggest that Torin1 is a highly selective inhibitor of mTOR when profiled against an extensive panel of serine/threonine, tyrosine, and lipid kinases.

Torin1 Causes Cell Cycle Arrest through a Rapamycin-resistant Mechanism That Is Also Independent of mTORC2—Our next goal was to test the role of mTOR signaling in normally growing cells. Rapamycin-mediated mTORC1 inhibition slows cell proliferation and reduces cell size, and so we suspected that dual mTORC1/2 inhibition would have similar but more severe effects (22). Indeed, wild-type MEFs treated with up to 500 nM rapamycin continued to proliferate, albeit at a reduced rate (Fig. 2A and supplemental Fig. S2). In contrast, 250 nM Torin1 completely inhibited proliferation (Fig. 2A and supplemental Fig. S2) and caused a G₁/S cell cycle arrest (Fig. 2B). Moreover, 250 nM Torin1 decreased cell size to a greater degree than 50 nM rapamycin (Fig. 2C). Based on the assumption that rapamycin completely disables mTORC1 kinase activity, we hypothesized that the enhanced effect of Torin1 was because of mTORC2 inhibition.

To test this hypothesis, we conducted identical experiments using MEFs that lack mTORC2 activity because Rictor has been deleted (16). We reasoned that Torin1 should have the same

effect as rapamycin on the proliferation and growth of these cells because mTORC2 is already inhibited. As in wild-type MEFs, rapamycin reduced but did not prevent proliferation (Fig. 2D). However, we were surprised to find that Torin1 continued to dramatically suppress proliferation and diminish cell size (Fig. 2, D–F), indicating that the differential effects of this compound with respect to rapamycin were not due to mTORC2 inhibition. Thus, mTOR has functions that are absolutely required for cell growth and proliferation and that are kinase-dependent, rapamycin-resistant, and independent of mTORC2.

Torin1 Disrupts mTORC1-dependent Phenotypes More Completely than Rapamycin—Despite the widely held assumption to the contrary, one explanation for our results is that rapamycin inhibits some but not all of the functions of mTORC1. To explore this possibility, we examined the effects of Torin1 on other processes besides growth and proliferation that are commonly associated with mTORC1 signaling. One such process is macroautophagy, often referred to simply as autophagy. Normally considered a response to starvation conditions, autophagy involves the formation of large double-membrane enclosed vesicles that engulf cytoplasmic contents, including both proteins and organelles (reviewed in Ref. 27). These vesicles then fuse with lysosomes to form autophagosomes that digest their contents, providing the cell with a source of amino acids and other nutrients when these are not available from the environment.

In yeast, rapamycin is a potent activator of autophagy (10). The situation is less clear in mammalian systems, where rapamycin alone is, at best, an inconsistent activator of autophagy and frequently requires combination with other PI3K/mTOR inhibitors, such as LY294002, or concomitant starvation for nutrients. We suspected that autophagy might also be regulated in part by rapamycin-resistant functions of mTORC1. A commonly used marker of autophagy is the protein light chain 3 (LC3), which translocates from the cytoplasm to autophagosomes where it is degraded when autophagy is induced (28). Using a green fluorescent protein-tagged LC3 construct, we found that Torin1 causes a strong re-localization of LC3 from the cytoplasm to autophagosomes in both wild-type and Rictor^{-/-} MEFs, whereas rapamycin caused only a minor change (Fig. 3A). Furthermore, we found that Torin1 treatment, like amino acid starvation, causes degradation of LC3B (LC3B-I) and transient accumulation of the faster running lipidated form (LC3B-II) in both MEFs and HeLa cells (Fig. 3B and supplemental Fig. S4A). An RNA interference-induced decrease in Raptor

FIGURE 1. Torin1 is a potent and selective mTOR inhibitor. A, Torin1 inhibits mTORC1 and mTORC2 *in vitro*. mTORC1 and mTORC2 were purified from HEK-293T stably expressing FLAG-Raptor and HeLa cells expressing FLAG-Protector-1, respectively. Following FLAG purification, each complex was subjected to *in vitro* kinase assays using S6K1 as a substrate for mTORC1 and Akt1 as a substrate for mTORC2. Assays were then analyzed by immunoblotting for the indicated proteins and phosphorylation states. B, Torin1 is an ATP-competitive inhibitor. The *in vitro* kinase activity of purified mTORC1 toward S6K1 was assayed in the presence of 20 nM Torin1 and increasing concentrations of ATP, as indicated. Assays were then analyzed by immunoblotting for the indicated proteins and phosphorylation states. C, Torin1 is a potent mTORC1 and mTORC2 inhibitor in cells. MEFs (p53^{-/-}) were treated with increasing concentrations of Torin1 or dual mTOR/PI3K inhibitors PI-103 and BEZ-235 for 1 h and then analyzed by immunoblotting for the indicated proteins and phosphorylation states. D, Torin1 has little effect on PI3K at concentrations where mTOR is completely inhibited. The experiment was performed as in C using mLST8-null MEFs and phosphorylation of Akt at Thr-308 was determined by immunoblotting. In mLST8-null MEFs, mTORC2 is inactive and Akt Ser-473 is constitutively dephosphorylated and so PDK1-mediated phosphorylation of Thr-308 only reflects PI3K activity. E, Torin1 is selective for mTOR over related kinases. IC_{50} values for Torin1 were determined using *in vitro* kinase assays for mTOR (3 nM), hVps34 (3 μM), PI3K- α (1.8 μM), DNA-PK (1.0 μM), and ATM (0.6 μM). IC_{50} values for PI-103 for mTOR (120 nM), PI3K- α (100 nM), DNA-PK (40 nM) were determined by the same assays. IC_{50} values for PI-103 for hVps34 (10 μM) and ATM (1.0 μM) were determined previously (21). F, Torin1 is selective for mTOR over other PI3K isoforms. EC_{50} values were determined for the indicated PI3K isoforms using the Invitrogen Adapta platform. The EC_{50} for mTOR was determined using the cell-based LanthaScreen platform.

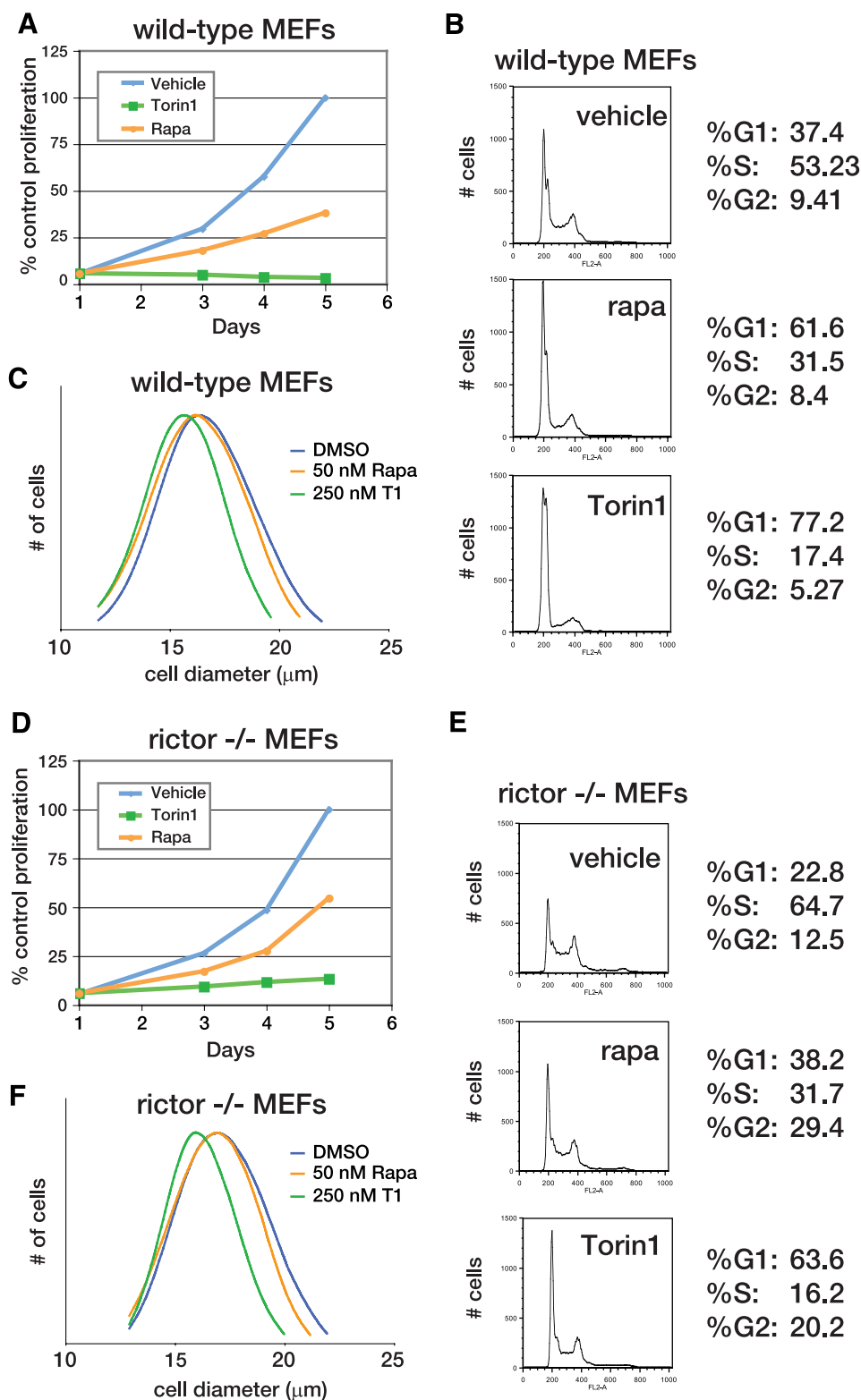


FIGURE 2. mTOR inhibition prevents cell growth and proliferation through an mTORC2-independent mechanism. *A*, mTOR inhibition by Torin1 but not rapamycin prevents the proliferation of wild-type MEFs. MEF ($p53^{-/-}$) cells were grown in the presence of vehicle (blue), 50 nM rapamycin (orange), or 250 nM Torin1 (green) for 4 days. Cell proliferation was measured in triplicate at indicated time points using the CellTiterGlo viability assay. *B*, Torin1 causes a G₁/S cell cycle arrest in wild-type MEFs. MEF ($p53^{-/-}$) cells were treated with vehicle (DMSO), 50 nM rapamycin (rapa), or 250 nM Torin1 for 48 h. Cells were then harvested, stained with propidium iodide, and analyzed by flow cytometry. *C*, normalized cell size distributions for Torin1 and rapamycin-treated wild-type MEFs. MEF ($p53^{-/-}$) cells were treated with vehicle (blue, mean 17.81 μm), 50 nM rapamycin (orange, mean 17.58), or 250 nM Torin1 (green, mean 16.46 μm) for 24 h. Cell sizes were measured using a particle counter and are displayed as a histogram. *D*, experiment was performed as in *A* using Rictor^{-/-}, p53^{-/-} MEFs. *E*, experiment was performed as in *B* using Rictor^{-/-}, p53^{-/-} MEFs. *F*, experiment was performed as in *C* using Rictor^{-/-}, p53^{-/-} MEFs. Cells were treated with vehicle (blue, mean diameter 17.85 μm), 50 nM rapamycin (orange, mean diameter 17.33 μm), or 250 nM Torin1 (green, mean diameter 16.24 μm).

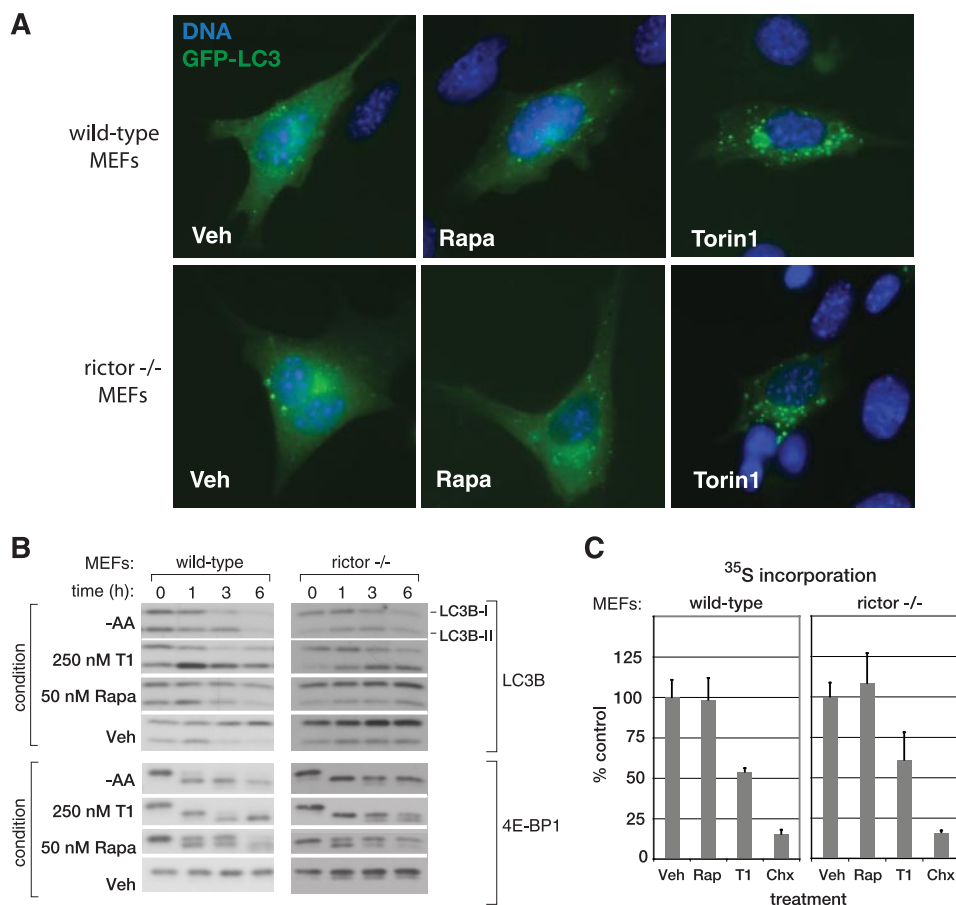


FIGURE 3. Torin1 inhibits mTORC1-dependent processes that are resistant to rapamycin. *A*, Torin1 but not rapamycin (*Rapa*) causes LC3 to relocate from the cytoplasm to autophagosomes. Wild-type ($p53^{-/-}$) or Rictor-null ($p53^{-/-}$) MEFs were transiently transfected with GFP-LC3 and treated with vehicle (*Veh*) (DMSO), 50 nM rapamycin, or 250 nM Torin1 for 3 h before being fixed and processed. Cells were also stained with Hoechst to visualize nuclei and imaged at $\times 63$. *B*, amino acid starvation and Torin1, but not rapamycin, cause LC3 degradation. Wild-type ($p53^{-/-}$) and Rictor-null ($p53^{-/-}$) MEFs were treated with vehicle (DMSO), 50 nM rapamycin, 250 nM Torin1 or grown in amino acid (AA)-free conditions for 0, 1, 3, or 6 h. Cells were lysed at the indicated time points and analyzed by immunoblotting. Induction of autophagy causes the degradation of the native LC3B (*LC3B-I*) protein and the transient accumulation of the faster running lipidated version (*LC3B-II*). *C*, Torin1 suppresses global protein synthesis through a rapamycin-resistant and mTORC2-independent process. Wild-type ($p53^{-/-}$) and Rictor-null ($p53^{-/-}$) MEFs were treated with vehicle (DMSO), 50 nM rapamycin (*Rap*), 250 nM Torin1, or 10 $\mu\text{g/ml}$ cycloheximide (*Chx*) for 2.5 h and then pulsed with ³⁵S-labeled methionine and cysteine for 30 min. The amount of ³⁵S incorporation was determined by scintillation counting. Measurements were made in triplicate, and error bars indicate standard deviation.

expression affected LC3 in a similar fashion as Torin1 treatment (supplemental Fig. S4B). Collectively, these results suggest that mTORC1 inhibition is sufficient to induce autophagy. Although the signaling mechanisms that connect mTORC1 to autophagy are currently unclear, ATP-competitive inhibitors, like Torin1, will likely reveal specific roles for mTORC1 that have been missed because of their insensitivity to rapamycin.

The mTORC1 pathway also has many connections to the regulation of cap-dependent translation. However, rapamycin often has only modest effects on rates of protein synthesis. To test whether Torin1 might inhibit protein synthesis more completely, we metabolically labeled cells using ³⁵S methionine/cysteine in the presence of either Torin1 or rapamycin. Surprisingly, whereas rapamycin had very little effect, Torin1 caused a nearly 50% decline in total protein synthesis in both wild-type and Rictor^{-/-} MEFs (Fig. 3C). As with autophagy, these results indicate that mTORC1 is a far more

important regulator of protein synthesis than experiments with rapamycin have indicated.

Rapamycin-resistant Functions of mTORC1 Are Required for Cap-dependent Translation—Because known mTORC1 substrates, S6K and 4E-BP1, are important regulators of mRNA translation, we next considered whether either is involved in the transduction of mTORC1-dependent but rapamycin-resistant functions. S6K activity has been shown to be completely inhibited by rapamycin treatment, and therefore we considered it unlikely to be the target of any rapamycin-resistant activity of mTORC1. 4E-BP1, however, is subject to a more complex regulatory process. The ability of 4E-BP1 to bind and inhibit eIF-4E is primarily regulated by the phosphorylation of four residues: Thr-37, Thr-46, Ser-65, and Thr-70. Phosphorylation of Thr-37 and Thr-46 is thought to be a priming event that permits the phosphorylation of the other two, thereby promoting dissociation from eIF-4E and permitting the formation of a functional eIF-4F complex (29). mTORC1 has been implicated in the regulation of 4E-BP1, but there are conflicting accounts of the importance of this connection as well as the underlying mechanism. For instance, mTORC1 phosphorylates the Thr-37 and Thr-46 sites *in vitro*, but these sites are considered rapamycin-insensitive in cells (30–32). Conversely, mTORC1 has

little effect *in vitro* on the phosphorylation of sites that are considered rapamycin-sensitive, Ser-65 and Thr-70. Moreover, a C-terminal motif in 4E-BP1, known as the TOR signaling motif and believed to mediate binding to mTORC1, and the N-terminal RAIP motif are required for phosphorylation of all sites (33–35). Finally, although rapamycin causes a substantial decrease in overall protein translation in some cell types (36), it has very little effect in others (13). A possible explanation is simply that rapamycin cannot completely inhibit mTORC1-dependent phosphorylation of 4E-BP1.

To test this hypothesis, we treated MEFs with increasing concentrations of either Torin1 or rapamycin and assessed the phosphorylation status of Thr-36, Thr-47, Ser-65, and Thr-70 by immunoblotting (Fig. 4A). Rapamycin completely prevented phosphorylation of S6K1 and caused a slight decrease in the phosphorylation of Ser-65 of 4E-BP1, but it had little effect on the phosphorylation of either Thr-37/46 or Thr-70 even at con-

Rapamycin-resistant Functions of mTORC1

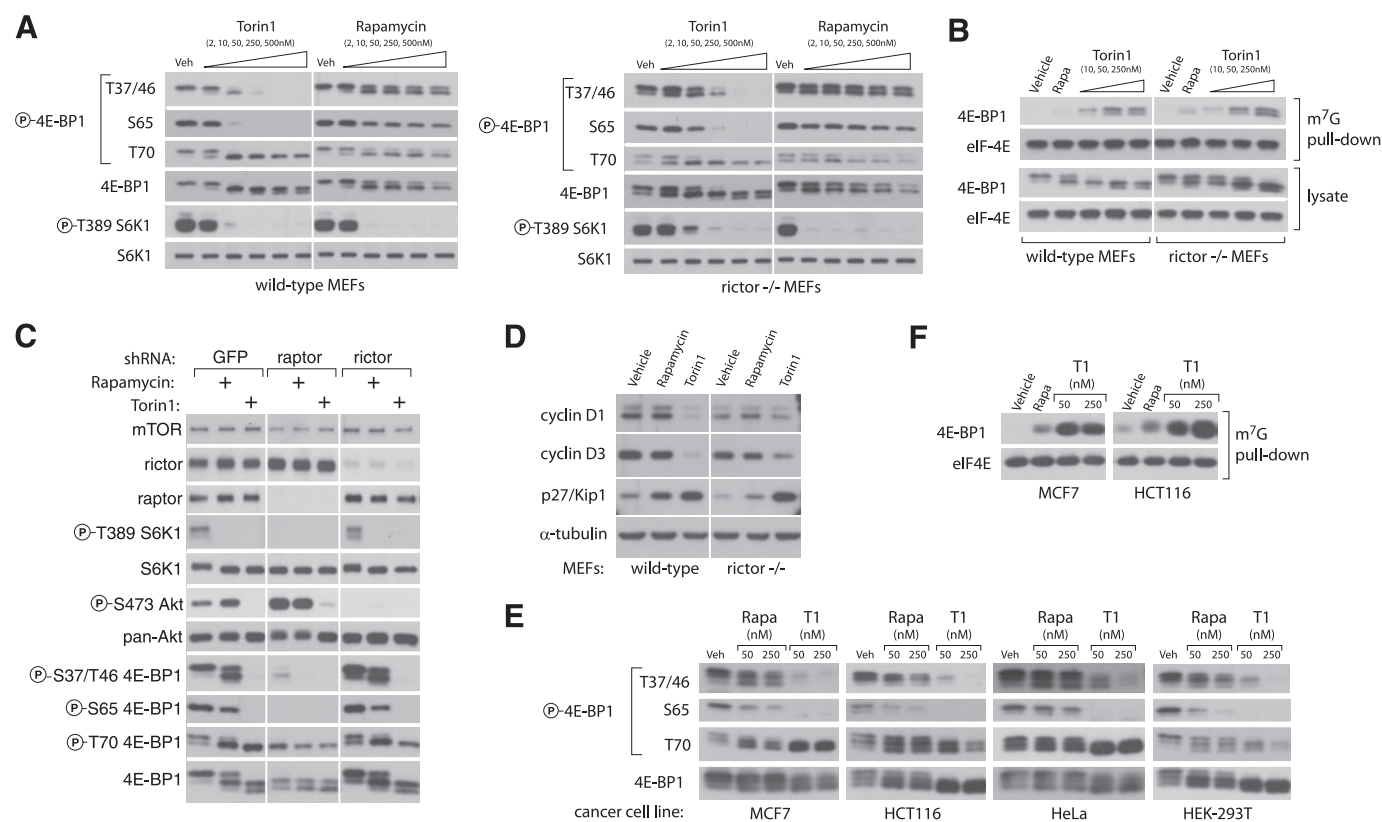


FIGURE 4. mTORC1 regulation of 4E-BP1 phosphorylation and binding to eIF-4E reveals rapamycin-resistant functions. *A*, phosphorylation of 4E-BP1 at Thr-37/46 and Ser-65 and binding to eIF-4E is dependent on mTORC1 but resistant to rapamycin. Wild-type ($p53^{-/-}$) and Rictor-null ($p53^{-/-}$) MEFs were treated with the indicated concentrations of Torin1 or rapamycin for 1 h and then lysed. Cell lysates were analyzed by immunoblot using antibodies specific for the indicated proteins or phosphorylation states. *B*, Torin1 increases the amount of 4E-BP1 bound to eIF-4E to a degree that far exceeds the effects of rapamycin. Wild-type ($p53^{-/-}$) and Rictor-null ($p53^{-/-}$) MEFs were treated with vehicle (DMSO), 50 nM rapamycin, or 250 nM Torin1 for 1 h before lysis. eIF-4E was purified from lysates using 7-methyl-GTP-Sepharose and analyzed by immunoblotting for the indicated proteins. *C*, phosphorylation of Thr-36/47 on 4E-BP1 requires Raptor but not Rictor. MEFs ($p53^{-/-}$) were infected with lentivirus expressing either control, Raptor-specific, or Rictor-specific shRNAs. Cells were grown for 4 days and then treated with vehicle (DMSO), 50 nM rapamycin, or 250 nM Torin1 for 1 h. Cell lysates were then analyzed by immunoblot using antibodies specific for the indicated proteins or phosphorylation states. *D*, prolonged mTOR inhibition alters the expression of key cell cycle regulators. Wild-type ($p53^{-/-}$) and Rictor-null ($p53^{-/-}$) MEFs were treated with vehicle (DMSO), 50 nM rapamycin, or 250 nM Torin1 for 48 h. Cell lysates were then analyzed by immunoblotting using antibodies specific for the indicated proteins. *E*, Torin1 prevents phosphorylation of rapamycin-resistant sites in human cancer cell lines. MCF7, HCT116, HeLa, and HEK-293T cell lines were treated with vehicle (Veh), rapamycin (Rap) (50 or 250 nM), or Torin1 (50 or 250 nM) for 1 h and then analyzed by immunoblotting for the indicated proteins and phosphorylation states. *F*, Torin1 increases the amount of 4E-BP1 bound to eIF-4E in human cancer cell lines. MCF7 and HCT116 cells were treated with vehicle (DMSO), 50 nM rapamycin, 50 nM Torin1, or 250 nM Torin1 for 48 h before lysis. eIF-4E was purified from lysates using 7-methyl-GTP-Sepharose and analyzed by immunoblotting for the indicated proteins.

concentrations as high as 500 nM, over 500 times greater than its IC_{50} value for inhibition of mTORC1 (Fig. 4A). In striking contrast, Torin1 substantially suppressed phosphorylation of Thr-37/46 and Ser-65 at concentrations as low as 10 nM and abolished it completely at 250 nM (Fig. 4A). Torin1 had nearly identical effects in Rictor-null MEFs, consistent with the hypothesis that these effects are because of inhibition of mTORC1 (Fig. 4A). Surprisingly, Thr-70 was unaffected by either Torin1 or rapamycin, supporting earlier predictions that it may be the target of a different kinase, such as Erk2 (37). Alternatively, it is possible that the Thr-70 4E-BP1 antibody is not phospho-specific. The dual-PI3K/mTOR inhibitors PI-103 and NVP-BEZ235 caused similar effects as Torin1 on 4E-BP1 phosphorylation (supplemental Fig. S3). Additionally, Torin1 had much greater effects than rapamycin on 4E-BP1 phosphorylation in a variety of human tumor cell lines, indicating that rapamycin resistance of mTORC1 is likely a general feature of most if not all mammalian systems (Fig. 4E). We next asked whether the increased dephosphorylation of 4E-BP1 by Torin1 led to increased association with eIF-4E. Using 7-methyl-GTP-

Sepharose to purify eIF-4E from cell lysates, we found that Torin1 causes substantially more binding of 4E-BP1 to eIF-4E than does rapamycin (Fig. 4, B and F). Torin1 did not affect the phosphorylation of eIF2 (supplemental Fig. S5).

Because the effects of Torin1 were nearly equivalent in wild-type and Rictor-null MEFs, we concluded that they could not be dependent on mTORC2. However, it remained possible that mTOR alone or an unidentified mTORC3 were responsible. To show that mTORC1 inhibition is sufficient to explain the effects of Torin1 on 4E-BP1 phosphorylation, we used RNA interference to knock down Raptor, an obligatory mTORC1 component, in wild-type MEFs (Fig. 4C). Depletion of Raptor in these cells suppressed Thr-37/46 and Ser-65 phosphorylation and 4E-BP1 mobility to a degree that equaled the effects of Torin1 and exceeded those of rapamycin, thereby supporting the conclusion that mTORC1, or at least a Raptor-containing mTOR complex, regulates 4E-BP1 phosphorylation through a rapamycin-insensitive kinase-dependent mechanism.

Defects in cap-dependent translation are also known to cause cell cycle arrest. This is thought to occur primarily through

decreased translation of cap-dependent mRNAs that encode factors that promote cell cycle progression, such as cyclin D1 and cyclin D3, and increased translation of cap-independent mRNAs that encode factors that suppress it, such as p27Kip1 (38–40). Moreover, recent work has shown that the depletion of cyclin D1 that is caused by amino acid starvation and rapamycin treated is mediated by 4E-BP1 (41). We suspected that the cell cycle arrest caused by Torin1 might be explained by changes in the abundance of these factors. Consistent with this, both wild-type and Rictor-null MEFs treated for 48 h with Torin1, but not rapamycin, had greatly depleted levels of cyclin D1 and D3, and a strong induction of p27/Kip1 (Fig. 4D). The ability of cells to recover from this arrest upon the removal of Torin1 was highly dependent on cell type (data not shown).

DISCUSSION

Rapamycin has been an indispensable tool throughout the history of TOR research and remains widely employed as a “complete” mTORC1 inhibitor in both research and clinical settings. Indeed, in yeast, it is a convincing mimic of the genetic inactivation of TORC1. In mammalian systems, most known mTOR substrates were discovered and validated using rapamycin as a pharmacological probe. Rapamycin forms a complex with the intracellular protein FKBP12, which then binds to the FRB domain of mTOR and inhibits phosphorylation of substrates through a poorly characterized mechanism. Although structural information is available for rapamycin in a complex with FKBP12 and the FRB domain of mTOR, it remains unclear how this prevents phosphorylation of direct mTOR kinase substrates (42). A model to explain our findings is that rapamycin blocks access to only a specific subset of mTORC1 substrates, whereas Torin1, because of its ATP-competitive mode of action, blocks phosphorylation of all. Additionally, as Torin1 is much smaller than FKBP12-rapamycin, it likely accesses its target site in mTOR-containing complexes more easily than FKBP12-rapamycin.

Re-interpretations of several recent studies support the notion that considerable mTORC1 functionality is resistant to rapamycin. Shor *et al.* (13) found that high concentrations (10 μ M) of rapamycin inhibit mTOR directly through an FKBP12-independent mechanism, suppressing both mTORC1 and mTORC2. Unlike the commonly used “low dose” (10–50 nM) and similarly to Torin1, “high-dose” rapamycin potently suppresses cap-dependent translation and inhibits proliferation in a wide variety of tumor cell lines. Although these authors concluded that these effects are because of mTORC2 inhibition, our findings indicate that they are more likely because of inhibition of rapamycin-resistant mTORC1-dependent functions. A study from Averous *et al.* (41) found that amino acid starvation caused a more complete depletion of cyclin D1 than rapamycin treatment and that this effect was mediated through 4E-BP1. Based on the assumption that rapamycin completely disables mTORC1, these authors concluded that amino acid starvation signals to 4E-BP1 through additional pathways besides mTORC1. We would suggest that it is more likely that amino acid starvation leads to a more complete inhibition of mTORC1 functions than does rapamycin. Finally, Choo *et al.* (43) found that phosphorylation sites on 4E-BP1 that are

acutely sensitive to rapamycin become re-phosphorylated in some cell lines after long periods of rapamycin treatment. Moreover, the recovery of 4E-BP1 phosphorylation depends on the mTORC1 component Raptor, leading the authors to conclude that prolonged rapamycin treatment confers on mTORC1 the capacity to phosphorylate 4E-BP1 in a rapamycin-resistant fashion. We find that mTORC1 likely has rapamycin-resistant functions in all cell lines (Fig. 4E). Because prolonged rapamycin treatment is known to hyperactivate the PI3K pathway, which is upstream of mTORC1, one possible explanation for the results of Choo *et al.* (43) is that rapamycin leads to the hyperactivation of the rapamycin-resistant functionality of mTORC1, effectively overcoming the partial inhibition caused by rapamycin.

Because many important features of TOR signaling are conserved between yeast and mammals, our finding that mTORC1 possesses cell-essential but rapamycin-resistant functions is unexpected. At the same time, our results indicate that the requirements for TORC1 signaling in maintaining protein synthesis and promoting cell division are more similar between yeast and mammalian systems than had been appreciated. Although we have focused on the rapamycin-insensitive regulation of 4E-BP1, we consider it likely that other similar mTORC1 substrates exist, particularly among the regulators of autophagy. The future combined use of Torin1 and phosphoproteomics will likely permit a more comprehensive assessment of all mTOR substrates. Given the current enthusiasm for rapamycin as a potential therapeutic, it is likely that ATP-competitive inhibitors of mTOR will have clinical utility as well.

Acknowledgments—We thank D. Kwiatowski (Harvard Medical School) for $p53^{-/-}/TSC2^{-/-}$ and $p53^{-/-}/TSC2^{+/+}$ MEFs; Christian Reinhardt (Massachusetts Institute of Technology) for $p53$ reagents; and Chris Armstrong (Invitrogen) for kinase profiling assistance. We also thank members of the Sabatini and Gray laboratories for helpful discussions and Ambit Biosciences for performing KinomeScan profiling.

REFERENCES

- Guertin, D. A., and Sabatini, D. M. (2007) *Cancer Cell* **12**, 9–22
- Manning, B. D., and Cantley, L. C. (2007) *Cell* **129**, 1261–1274
- Sehgal, S. N. (2003) *Transplant. Proc.* **35**, S7–S14
- Sarbassov, D. D., Ali, S. M., Sengupta, S., Sheen, J. H., Hsu, P. P., Bagley, A. F., Markhard, A. L., and Sabatini, D. M. (2006) *Mol. Cell* **22**, 159–168
- Richter, J. D., and Sonenberg, N. (2005) *Nature* **433**, 477–480
- Holz, M. K., Ballif, B. A., Gygi, S. P., and Blenis, J. (2005) *Cell* **123**, 569–580
- Raught, B., Peiretti, F., Gingras, A. C., Livingstone, M., Shahbazian, D., Mayeur, G. L., Polakiewicz, R. D., Sonenberg, N., and Hershey, J. W. (2004) *EMBO J.* **23**, 1761–1769
- Shahbazian, D., Roux, P. P., Mieulet, V., Cohen, M. S., Raught, B., Taunton, J., Hershey, J. W., Blenis, J., Pende, M., and Sonenberg, N. (2006) *EMBO J.* **25**, 2781–2791
- Barbet, N. C., Schneider, U., Helliwell, S. B., Stansfield, I., Tuite, M. F., and Hall, M. N. (1996) *Mol. Biol. Cell* **7**, 25–42
- Noda, T., and Ohsumi, Y. (1998) *J. Biol. Chem.* **273**, 3963–3966
- Neshat, M. S., Mellinshoff, I. K., Tran, C., Stiles, B., Thomas, G., Petersen, R., Frost, P., Gibbons, J. J., Wu, H., and Sawyers, C. L. (2001) *Proc. Natl. Acad. Sci. U. S. A.* **98**, 10314–10319
- Pedersen, S., Celis, J. E., Nielsen, J., Christiansen, J., and Nielsen, F. C. (1997) *Eur. J. Biochem.* **247**, 449–456
- Shor, B., Zhang, W. G., Toral-Barza, L., Lucas, J., Abraham, R. T., Gibbons,

- J. J., and Yu, K. (2008) *Cancer Res.* **68**, 2934–2943
14. Takeuchi, H., Kondo, Y., Fujiwara, K., Kanzawa, T., Aoki, H., Mills, G. B., and Kondo, S. (2005) *Cancer Res.* **65**, 3336–3346
 15. Sabatini, D. M. (2006) *Nat. Rev. Cancer* **6**, 729–734
 16. Guertin, D. A., Stevens, D. M., Thoreen, C. C., Burds, A. A., Kalaany, N. Y., Moffat, J., Brown, M., Fitzgerald, K. J., and Sabatini, D. M. (2006) *Dev. Cell* **11**, 859–871
 17. Moffat, J., Grueneberg, D. A., Yang, X., Kim, S. Y., Kloepfer, A. M., Hinkle, G., Piquani, B., Eisenhaure, T. M., Luo, B., Grenier, J. K., Carpenter, A. E., Foo, S. Y., Stewart, S. A., Stockwell, B. R., Hacohen, N., Hahn, W. C., Lander, E. S., Sabatini, D. M., and Root, D. E. (2006) *Cell* **124**, 1283–1298
 18. Ali, S. M., and Sabatini, D. M. (2005) *J. Biol. Chem.* **280**, 19445–19448
 19. Sarbassov, D. D., Guertin, D. A., Ali, S. M., and Sabatini, D. M. (2005) *Science* **307**, 1098–1101
 20. Sancak, Y., Thoreen, C. C., Peterson, T. R., Lindquist, R. A., Kang, S. A., Spooner, E., Carr, S. A., and Sabatini, D. M. (2007) *Mol. Cell* **25**, 903–915
 21. Knight, Z. A., Gonzalez, B., Feldman, M. E., Zunder, E. R., Goldenberg, D. D., Williams, O., Loewith, R., Stokoe, D., Balla, A., Toth, B., Balla, T., Weiss, W. A., Williams, R. L., and Shokat, K. M. (2006) *Cell* **125**, 733–747
 22. Nobukuni, T., Joaquin, M., Rocco, M., Dann, S. G., Kim, S. Y., Gulati, P., Byfield, M. P., Backer, J. M., Natt, F., Bos, J. L., Zwartkruis, F. J., and Thomas, G. (2005) *Proc. Natl. Acad. Sci. U. S. A.* **102**, 14238–14243
 23. Brunn, G. J., Williams, J., Sabers, C., Wiederrecht, G., Lawrence, J. C., Jr., and Abraham, R. T. (1996) *EMBO J.* **15**, 5256–5267
 24. Maira, S. M., Stauffer, F., Brueggen, J., Furet, P., Schnell, C., Fritsch, C., Brachmann, S., Chene, P., De Pover, A., Schoemaker, K., Fabbro, D., Gabriel, D., Simonen, M., Murphy, L., Finan, P., Sellers, W., and Garcia-Echeverria, C. (2008) *Mol. Cancer Ther.* **7**, 1851–1863
 25. Biondi, R. M., Kieloch, A., Currie, R. A., Deak, M., and Alessi, D. R. (2001) *EMBO J.* **20**, 4380–4390
 26. Scheid, M. P., Marignani, P. A., and Woodgett, J. R. (2002) *Mol. Cell. Biol.* **22**, 6247–6260
 27. Mizushima, N., Levine, B., Cuervo, A. M., and Klionsky, D. J. (2008) *Nature* **451**, 1069–1075
 28. Kabeya, Y., Mizushima, N., Ueno, T., Yamamoto, A., Kirisako, T., Noda, T., Kominami, E., Ohsumi, Y., and Yoshimori, T. (2000) *EMBO J.* **19**, 5720–5728
 29. Gingras, A. C., Gygi, S. P., Raught, B., Polakiewicz, R. D., Abraham, R. T., Hoekstra, M. F., Aebersold, R., and Sonenberg, N. (1999) *Genes Dev.* **13**, 1422–1437
 30. Burnett, P. E., Barrow, R. K., Cohen, N. A., Snyder, S. H., and Sabatini, D. M. (1998) *Proc. Natl. Acad. Sci. U. S. A.* **95**, 1432–1437
 31. Fingar, D. C., Richardson, C. J., Tee, A. R., Cheatham, L., Tsou, C., and Blenis, J. (2004) *Mol. Cell. Biol.* **24**, 200–216
 32. Wang, X., Beugnet, A., Murakami, M., Yamanaka, S., and Proud, C. G. (2005) *Mol. Cell. Biol.* **25**, 2558–2572
 33. Choi, K. M., McMahon, L. P., and Lawrence, J. C., Jr. (2003) *J. Biol. Chem.* **278**, 19667–19673
 34. Schalm, S. S., Fingar, D. C., Sabatini, D. M., and Blenis, J. (2003) *Curr. Biol.* **13**, 797–806
 35. Tee, A. R., and Proud, C. G. (2002) *Mol. Cell. Biol.* **22**, 1674–1683
 36. Beretta, L., Gingras, A. C., Svitkin, Y. V., Hall, M. N., and Sonenberg, N. (1996) *EMBO J.* **15**, 658–664
 37. Herbert, T. P., Tee, A. R., and Proud, C. G. (2002) *J. Biol. Chem.* **277**, 11591–11596
 38. Albers, M. W., Williams, R. T., Brown, E. J., Tanaka, A., Hall, F. L., and Schreiber, S. L. (1993) *J. Biol. Chem.* **268**, 22825–22829
 39. Jiang, H., Coleman, J., Miskimins, R., and Miskimins, W. K. (2003) *Cancer Cell Int.* **3**, 2
 40. Rosenwald, I. B., Lazaris-Karatzas, A., Sonenberg, N., and Schmidt, E. V. (1993) *Mol. Cell. Biol.* **13**, 7358–7363
 41. Averous, J., Fonseca, B. D., and Proud, C. G. (2008) *Oncogene* **27**, 1106–1113
 42. Choi, J., Chen, J., Schreiber, S. L., and Clardy, J. (1996) *Science* **273**, 239–242
 43. Choo, A. Y., Yoon, S. O., Kim, S. G., Roux, P. P., and Blenis, J. (2008) *Proc. Natl. Acad. Sci. U. S. A.* **105**, 17414–17419